CHAPTER – 3

PROTONATION-DEPROTONATION EQUILIBRIUM OF OH GROUPS OF BIOLOGICALLY IMPORTANT INDICATOR MOLECULES IN MICELLAR MEDIA

3.1. Introduction and review of previous works

Surfactants, some times called surface active agents or detergents, are materials that contain both apolar, hydrophobic (lipophobic) and polar, hydrophilic (lipophobic) groups[1-8]. In solvents which have a strong three dimensional structure, for example water, hydrazine, 1,2-diols[9-12] or sulphuric acid[13] this dual character of the amphiphile leads to self association or micellization. In the small colloidal particles, or micelles, which result, the apolar groups tend to pack together away from the polar solvents, and the polar or ionic head groups tend to be at the surface of the micelle where they interact with the solvent. Water is the preferred solvent for study of this phenomenon and all the results discussed in this chapter relate to experiments in water unless otherwise specified. Micellization is a manifestation of the strong self – association of water and similar solvents and is an example of the hydrophobic or solvophobic effect (the term applies to the interactions in a variety of associated solvents other than water), which forces self-association of apolar materials.[14] Micelles are small, relative to the wavelength of light. Their solutions are therefore transparent, but they scatter light, and this properly provided compelling evidence for the formation or discrete micelles.[15,16]

Most studies of micellar systems have been carried out on synthetic surfactants where the polar or ionic head group may be cationic, e.g., an ammonium or pyridinium ion, anionic, e.g., a carboxylate, sulphate or sulfonate ion, non ionic, e.g., hydroxyl compound, or zwitterionic, e.g., an amine oxide or a carboxylate or sulfonate.[3] Some of surfactants used in the present study are listed in Table 1, together with values of critical micelle concentration, cmc. This is the surfactant concentration at the onset of micellization[17] and can therefore be taken to be the maximum concentration of monomeric surfactant in a solution.[18] Its value is related to the change of free energy on micellization.[3-5]

TABLE: 1

Synthetic surfactants	cmc/M
Cetyltrimethylammonium bromide (CTAB)	9.0×10^{-4}
Sodium dodecylsulfate (SDS)	8.0×10^{-3}
Sodium bis(2-ethylhexylsulfosuccinate), Aerosol-OT (AOT)	2.5×10^{-3}
Polyoxyethylenesorbitan monopalmitate (Tween – 40)	3.6×10^{-5}
Polyoxyethylenelauryl ether (Brij-35)	4.8×10^{-5}

Micellization depends upon a balance of forces and the cmc decreases with the increasing hydrophobicity of the apolar groups, and for ionic amphiphile also depends upon the nature and concentration of counter ions in solution. Added electrolytes decrease the cmc, and the effect increases with decreasing charge density of the counter ion. Divalent counter ions, however, lead lower values of cmc than do univalent ions because ion binding, of itself lead to a decrease in entropy.[19] Non-ionic and zwitterionic amphiphiles typically have lower values of the cmc than otherwise similar amphiphiles, because there is no formal coulombic repulsion between the head groups.

Ionic surfactants form approximately spherical micelle in water with ionic head groups at the surface and counter ions clustered around the micelle partially neutralizing the charges. Counter ions which are closely associated with the micelle can be assumed to be located in shell, the so called stern layer, the thickness of which should be similar to the size of the micellar head groups. The ionic head groups will repel monomeric co-ions. The hydrophobic alkyl groups pack randomly and parts of the chains are exposed to water at the surface.

The cmc is a key property, because it is related to free energy difference between monomer and micelles. The onset of micellization is detected by

marked changes in such properties as surface tension, refractive index and conductivity (for ionic micelles); light scattering also increases sharply on micellization, as does solubilization of hydrophobic solutes. To a first approximation the solution can be assumed to contain monomeric amphiphiles and fully formed micelles with sub-micellar particles playing a minor role. It has long been known that aqueous micelles can influence chemical rates and equilibrium,[1,20-22] and there are a number of related self assembling colloids which share this ability. Microemulsions generally contain water, an oil, a surfactant and a co-surfactant which is generally a medium chain length alcohol, amine or similar polar organic molecule.[23,24] Oil in water (o/w) microemulsions are formed when water is the bulk solvent. The droplets are larger than normal micelles in water[25,23] but the two structures have the common feature that the polar or ionic head groups are in contact with water. Water in oil (w/o) microemulsions are formed when oil is the bulk solvent. They are akin to the reverse microemulsions, which form when surfactants, usually with small amount of water, are dissolved in an apolar organic solvent.[3,26] The interiors of these droplets contain water and the apolar regions of the emulsions are in contact with the apolar solvent.[27] Micelles in water have long been known to influence acid-base indicator equillibria and the effects were rationalized in term of Hartley's Rules which related change in equilibrium constants to micellar charge.[1] These rules were subsequently applied to micellar effects upon the rates of attack of OH^- upon triarylmetheyl dye cations.[20,28] These early studies of micelles effects upon reaction rates and equilibrium are described in an extensive monograph.[3] The original work on ionic reactions was in normal micelles in water, but subsequently there has been extensive work on reactions in reverse micelles.[28-32] There has also been a great deal of work on photochemical and radiation induced reactions in a variety of colloidal systems, and microemulsions have been used as a media for a variety of thermal, electrochemical and photochemical reactions.[4,24,33]

Much of the impetus for the study of reactions in micelles is that they model, to a limited extent, reaction in biological assemblies. Synthetic vesicles and cyclodextrins are other model reaction media and the term "Bio-mimetic Chemistry" has been coined to describe this general area of study. Work in this area is reviewed in recent publications.[4,8]

Hartley showed that micellar effects upon acid-base indicator equilibrium could be related to the ability of anionic micelles to attract, and cationic micelles to repel hydrogen ions. More recently attempts have been made to qualify these ideas in terms of the behaviour of a micelle as a sub-microscopic solvent, together with an effect due to its surface potential.[34]

Unique property of micelles is that it is a microheterogeneous system possessing an interior organic solvent like phase and an exterior aqueous phase. This feature leads to the enhanced micelles solubilization of both nonpolar and polar compounds of wide variety. Even large bio-molecules, viz. DNA, RNA, proteins are soluble in micelles. Solubilization of the substrates in micellar media can modify their equilibrium and kinetic properties.[35-39] Inherited surface charge of ionic micelles under favourable conditions help their association with reacting substances. In the case of non-ionic micelles selective extraction by hydrophobic forces of the reagents may help their compartmentalization[40-44] in micelles. The micellar catalyzed reactions are explained in terms of lowering of activation energy,[45] fractal dimension[46-48] decreased in the degree of freedom of their reactants by way of their immobilization in the diffusion phase space of micelles.[45] The knowledge on the acid-base equilibrium of substrates in micellar media is required in relation to their potential for analytical application, as spectroscopic probes, as catalysts etc. The solubilisates in micelles are often analogically modeled as equivalent to membranes and enzymes.

As has already been mentioned, micelles have the ability to solubilize a wide range of inorganic and organic compounds. The water solubility of non-polar organic compounds can be remarkably increased in micelles media. The

water pools of reverse micelles can solubilize larger molecules like DNA, RNA etc. The different solubilization sites of micelles have been experimentally verified by using spectroscopic and other methods.[34,49-52] The solubilization sites have different micro-polarity. The solubilisates get adsorbed at the sites of micelles depending on their nature. The hydrocarbons having no polar groups, in small concentration get solubilized in micellar hydrocarbon core. In the stern layer, the solubilisates reside associated with the polar/charged head groups of the surfactants. The repulsive interaction between the surfactant head groups is reduced resulting in the increased stability of the organic compounds having polar/ionic group. Highly polar or charged molecules may reside just outside the stern layer. In organic ions as well as counter ions are found in this site. The site that is further away from the stern layer are generally occupied when water-soluble substrates are taken in excess and the capacities of the first three sites are full. The site for solubilization thus depends on the nature of both the solubilisate and the micelles.

The polarity of the micelles microenvironment has been investigated using various probes.[53-60] The hydrocarbon core of micelles has very low polarity, similar to hydrocarbon solvents (dielectric constant 2-4). However, the stern layer is much more polar due to the presence of charged or polar head groups of surfactants. For charged micelles the stern layer contains charged head groups as well as a fraction of counter ions attached to the head group and so is more polar than non-ionic micelles. Fluorescence studies with probe molecules have shown penetration of a significant amount of water molecules into the hydrocarbon. The polarity gradually decreases from stern layer to the interior hydrocarbon region. Outside the stern layer, the polarity rapidly reaches the value of the bulk solvent. For normal micelles this bulk solvent is water with dielectric constant 80; for reverse micelles it is the organic solvent of low dielectric constant.

Organic compounds are soluble in micellar media although they may or may not be soluble in water or organic solvent alone. This solubilization leads

to a change in the acid-base equilibrium. In general, two established models, viz, thermodynamic model and the pseudophase ion exchange model, explain the observed pK_a shifts of the acid-base equilibrium. The thermodynamic model qualitatively explains the pK_a shifts and is thus simple and the most widely used model. The pseudo-phase ion-exchange model although can explain the pK_a shifts both qualitatively and quantitatively, is less popular for its inherent complexity. Both models are discussed below, briefly.

1. Thermodynamic model:

The pK_a values of a substrate are expected to be different in the three different types of micelles (cationic, anionic and non-ionic) because the micellar surface charge influence the acid-base equilibrium. The shift in the acid-base equilibrium is mainly guided by two factors.

(i) Due to the change in the polarity of the slubilization site of the micelle compared to the bulk solvent. This is commonly known as micro-environment or medium effect.

(ii) Due to the influence of the electrostatic potential present at the micellar solubilization site, commonly known as potential effect.

The site of solubilization of the molecule has considerable influence on the shift of the acid-base equilibrium. At low concentration of the substrate, the strongest sites will be occupied, but at higher concentration, both the strong and weak sites will be occupied. Thus the observed shift of the acid-base equilibrium depends also on the substrate concentration.

The successive acid-base equilibria of a solubilisate can be represented by the following general equillibria :

$$A^{+n} = B^{+(n-1)} + H^{+} \qquad (1)$$

where n=0, 1,2 etc. For a titration experiment of a completely micelle bound solubilisate, one measures the proton activity in the bulk phase and the

concentration ratio of acidic and basic forms of the solubilisates and the micelles. Thus the apparent acid-base equilibrium K_a^A is characterized by

$$K_a^A = [B_m]\,[H_w]/[A_m] \qquad (2)$$

In other words, pK_a^A is the bulk pH for which the indicator (probe molecule) in the micelle will release 50% of its H^+ ion in water. Here $[A_m]$ and $[B_m]$ represents the concentrations of the micelle bound acidic and basic form of the indicator and $[H_w]$ are the bulk hydrogen ion concentration. If we consider that A and B forms of the solubilisate are completely micelle bound and then concentrations are so low that the activities can be replaced by concentrations, then we can write[34] :

$$pK_a^i - pK_a^w = \Delta pK_a^i = \{(\mu_B^m - \mu_A^w) - (\mu_A^m - \mu_A^w)\}\ 2.3RT \qquad (3)$$

and

$$pK_a^{mw} - pK_a^w = \Delta pK_a^{mw} = \Delta\, pK_a^i - F\psi/\ 2.3RT \qquad (4)$$

where K_a^w, K_a^i and K_a^{mw} are the dissociation constants of the solubilisate in water, in non-ionic micelle and charged micelle respectively. Here μ is the chemical potential, ψ is the electrical potential and R, T and F have their usual meaning.

Equation (3) can explain qualitatively the origin of shift of pK_a values in non-ionic micelle compared to water. There lie three possibilities about the charge of A and B in most cases:

i) A is charged and B is neutral.

ii) A is neutral and B is charged

iii) Both A and B are charged.

If A or B is charged, then it is more stable in water than in the organic phase like micellar sites and so, $(\mu^m - \mu^w)$ will be positive. However, uncharged organic solubilisate is more stable in micellar phase than in water and so

$(\mu^m - \mu^w)$ is expected to be negative. Thus a resultant positive ΔpK_a^i is expected when B is charged and A is uncharged, and a resultant negative ΔpK_a^i is expected when A is charged but B is uncharged. In other words, the equilibrium is shifted to right for (i) and the equilibrium will be shifted to left for (ii).

Case (iii) occurs generally for the successive dissociation of an acid or a base. In this case, B will have charge higher than A. In this case, $(\mu^m - \mu^w)$ will be positive for A and B but will be higher in magnitude for B, as higher charged solubilisate will be more unstable at the micellar interface. As a result, pK_a will be negative in most cases. However, above explanation can never be generalised.

2. Pseudophase Ion Exchange (PIE) model:

A major shortcoming of the thermodynamic model is that it does not account for the generally observed specific counter ion effect on the micelle induced pK_a shifts. PIE model successfully explain this fact by considering specific ion-exchange constants. This model is used to represent the acid-base equilibrium in ionic micelle. The basic assumptions of the model are as follows:

(i) Micelles act as a separate phase, homogeneously distributed throughout the solution and the medium property of this phase is independent of solution composition.

(ii) Ionization of micelle bound substrate is described by a intrinsic acidity constant that reflects the medium property of micelle.

(iii) Total concentration of counter ions at the micellar interface is constant and independent of the surfactant concentration and the type of counter ion.

(iv) The distribution of counter ions between micelles and water is described by an empirical ion-exchange constant that reflects the different specific interactions of the counter ions.

There are several reviews and papers dealing with the theory of PIE model and its application.[61-64] According to PIE model, the shift of pK_a values in charged micelles compared to pK_w is explained by considering the transfer of conjugate acid-base forms of the solubilisate and H^+/OH^- ion from large volume of water into the much smaller volume of micellar pseudo-phase. Addition of salt in anionic micelle results in the displacement of H^+ ion from micellar surface to water by the cations of the added salts. As a result, the H^+ ion concentration in micelle surface decreases with the addition of salt and so a decrease in pK_a is observed. Similarly, in cationic micelles, OH^- ions are replaced from the micellar interface by the anion of the added salts and thus OH^- concentration in micellar interface decreases compared to that in the bulk water.

For the last four decades a considerable amount of research effort has been directed toward determining the physicochemical properties of self-assembled surfactant aggregates, especially micelles and unilamellar vesicles. Although many reasons can be cited for the widespread interest in elucidating the physicochemical properties of micelles and vesicles, there are primarily three reasons. Firstly, one can consistently and easily prepare aqueous micellar and vesicular solutions which have aggregates of colloidal dimensions with characteristic size, shape and surface properties. Hence, micellar and vesicular systems have been employed as model systems in investigations concerned with understanding colloidal physicochemical phenomena.[35,65] Secondly, the similarities between self-assembled surface aggregates, such as micelles, vesicles and biological lipid membranes have been noted. Thus, in many studies, micelles and vesicles have served as rudimentary model systems for biological lipid membrane systems.[4,35] Thirdly, it has been found that micelles and vesicles can act as unique reaction media. Indeed, solubilization of reactants within self-assembled surfactant aggregates frequently leads to alter reaction rates, reaction routes and stereochemistry[4,35]. Obviously, micelles and

vesicles cannot be fully exploited as reaction media until all their physicochemical properties have been ascertained.

Spectroscopic techniques based on either the optical absorption or the emission of light from a specific aromatic probe molecule has been often used to determine certain physicochemical properties of micelles and vesicles.[66] In some cases, spectroscopic probe techniques provide the only means of ascertaining a particular physicochemical property, while in other cases, the simplicity of application has resulted in a spectroscopic probe technique being employed in preference to a more classical colloidal measurement, such as light scattering, osmometry or conductivity.

The majority of spectroscopic probes used in studying the physicochemical properties of self-assembled surfactant systems are aromatic derivatives. Data on the time averaged sites of solubilization in an amphiphilic aggregate are obtained mainly from fluorescence, uv/vis absorption and nmr spectroscopy[3,67,72]. However, from the literature, it appears that 'free' aromatic probes are solubilized on average at the water/hydrocarbon interface of most micelles, and may be present at either the water/hydrocarbon interface or in the interior of the hydrocarbon bilayer of vesicles. Mukerjee[68,69] has indicated that the main reasons for 'free' aromatic molecules residing on average at the micelle/water interface stems from (i) the pronounced surface activity of aromatic species at the hydrocarbon/water interface, (ii) the high Laplace pressure of the micelle cores, and (iii) the high effective interfacial volume of a micellar structure. Specific interactions between the aromatic molecules and surfactant headgroups may also play an important role. It is generally well established that such interactions exist if the head group is a quaternary ammonium group.[70-72]

Acid-Base Equilibria.

The acid-base equilibrium of an indicator, which has its prototropic moiety residing within the interfacial region of a self-assembled surfactant aggregate, can be represented as

$$HIN_i^z \rightleftharpoons^{K_a^i} H_i^+ + IN_i^{z-1} \quad (5)$$

and the thermodynamic acid-base equilibrium constant for this reaction, K_a^i, is given by

$$K_a^i = (a_{H^+}^i \, a_{IN}^i) / a_{HIN}^i \quad (6)$$

where superscript z is the charge on the protonated form of the indicator, subscript or superscript i denotes the interfacial region, and $a_{H^+}^i$, a_{IN}^i, and a_{HIN}^i are the activities of the various species involved in the equilibrium.

There is no direct experimental method for determining $a_{H^+}^i$, and as a result K_a^i cannot be determined by any direct means. Nevertheless, it is possible by experiment to study an apparent acid-base equilibrium for an interfacially located prototropic moiety of an indicator, i.e.

$$HIN_i^z \rightleftharpoons^{K_a^{obs}} H_w^+ + IN_i^{z-1} \quad (7)$$

and equilibrium constant of this reaction,

$$K_a^{obs} = (a_{H^+}^w \, [IN^{z-1}]_i) / [HIN^z]_i \quad (8)$$

where subscript or superscript w denotes the bulk aqueous solution and $[IN^{z-1}]_i$ and $[HIN^z]_i$ are the interfacial concentrations of the conjugate base and conjugate acid forms of the indicator, respectively. According to Boltzmann's law, the hydrogen ion activity at a point in the vicinity of a charged interface and the hydrogen ion activity in the bulk aqueous solution are related by

$$a_{H^+}^i = a_{H^+}^w \exp\left(\frac{-e\psi}{kT}\right) \quad (9)$$

where e is the unit electronic charge, k is the Boltzmann constant, T is the absolute temperature, and ψ is the electrostatic mean field potential at the point

being considered.[73] Therefore the apparent pK_a, pK_a^{obs}, is related to the thermodynamic intrinsic interfacial pK_a, pK_a^i, through the expression

$$pK_a^{obs} = pK_a^i + \log\frac{\gamma_{IN}^i}{\gamma_{HIN}^i} - \frac{e\psi}{2.303kT} \qquad (10)$$

where γ_{IN}^i and γ_{HIN}^i denote the activity coefficients of the conjugate base and conjugate acid forms of the indicator, respectively, referred to the interfacial phase at infinite dilution. Generally it is assumed that

$$pK_a^0 = pK_a^i + \log\frac{\gamma_{IN}^i}{\gamma_{HIN}^i} \qquad (11)$$

so that

$$pK_a^{obs} = pK_a^0 - \frac{e\psi}{2.303kT} \qquad (12)$$

where ψ is the mean field potential at the time-averaged location of the prototropic moiety of the indicator in the interfacial region. Note that if the prototropic moiety resides on average in the plane of the surface charge then the mean field potential in equation 12 is the surface potential, ψ_0. Fromherz and co-workers[34,74] have shown that there is also a thermodynamic route by which equation 12 can be derived.

Providing (i) there are no specific molecular interactions or "salt effects" which significantly interfere with the intrinsic interfacial acid-base equilibrium of an indicator, and (ii) the mean solvent characteristics of interfacial microenvironments can be mimicked by organic solvent/water mixtures, then there is a connection between the pK_a^0 values of the indicator situated in self-assembled surfactant aggregates and the pK_a values of the indicator in organic solvent/water mixtures.[34,75-78]

The acid-base equilibrium of an indicator in an organic solvent/water mixture (m) can be represented as

$$HIN_m^z \rightleftharpoons^{K_a^m} H_m^+ + IN_m^{z-1} \qquad (13)$$

with equilibrium constant in the mixture,

$$K_a^m = (a_{H^+}^m a_{IN}^m) / a_{HIN}^m \qquad (14)$$

To enable a thermodynamically correct comparison to be made between the results of organic solvent/water pH titrations and the pH titrations performed in self-assembled surfactant solution, it is necessary to convert the one-phase pK_a^m values into two-phase pK_a^0 values. This can be accomplished by making two main assumptions. The first assumption is that the concentration ratio $[IN^{z-1}]_i / [HIN^z]_i$ is equivalent to the activity ratio a_{IN}^m / a_{HIN}^m in an organic solvent/water mixture with the same dielectric constant as the interfacial dielectric constant (D_{eff}) value where the protonatable portion of the indicator resides on average. With this assumption

$$pK_a^0 = pK_a^m - \log {}_m\gamma_{H^+} \qquad (15)$$

where ${}_m\gamma_{H^+}$ is the medium effect on the proton. Since ${}_m\gamma_{H^+}$ is defined in terms of single ion activity coefficients it cannot be determined by thermodynamic means. Hence one makes the second assumption, namely that ${}_m\gamma_{H^+}$ values can be approximated by the values of the medium effect on HCl in organic solvent/water mixtures, ${}_m\gamma_{\pm}$. In this manner a reference pK_a^0 curve as a function of dielectric constant can be acquired from the pK_a^m values for an indicator. The reference pK_a^0 curve as a function of dielectric constant can then be used in conjunction with the pK_a^0 values obtained from the indicator in self-assembled surfactant aggregates to estimate D_{eff} values for the interfacial regions.

The pK_a^0 values of a number of acid-base indicators in some self-assembled surfactant aggregates are known to be influenced by specific

molecular interactions and/or interfacial "salt-effect".[75,83] The pK_a^0 values measured in these indicator/surfactant aggregate systems cannot validly be compared with a reference organic solvent/water pK_a^0 versus dielectric constant curve.[79]

In the present study, a few biologically important organic molecules viz., some aromatic amino acids and derivatives of amino acids and also naphthols are chosen for monitoring the protonation-deprotonation equilibria of the hydroxy groups in 1,4-dioxane-water mixture, as well as in non-ionic and charged micelles. These organic compounds are of biological relevance and the derivatives are, 5-Hydroxyindole, 5-Hydroxy-L-tryptophan, L-Tyrosine, L-Tyrosinemethylester, 1-Naphthol and 2-Naphthol.

Among the indicator molecules in the above list, first two posses similar structures, while the third and fourth are otherwise identical except the fact that the fourth one does not form carboxylate anion at high pH. The structures of these pH indicator molecules are given below:

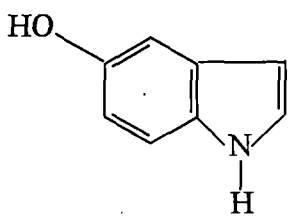

5-Hydroxyindole

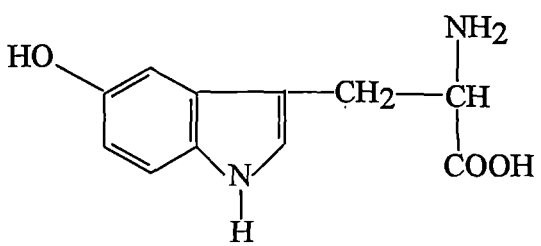

5-Hydroxy-L-tryptophan

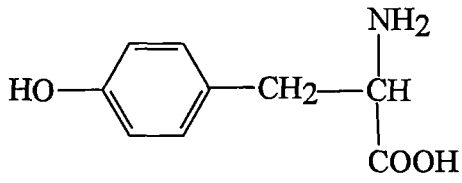

L-Tyrosine

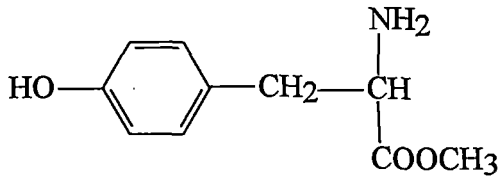

L-Tyrosinemethylester

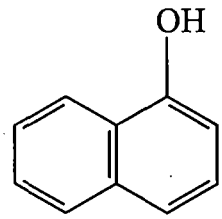

1–Naphthol

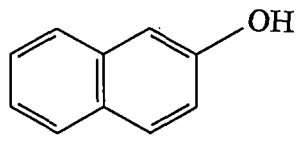

2–Naphthol

Apart from the biomolecules, and their derivatives, 1- and 2-Naphthols are also included in the above list as pH indicators because due to the presence of the hydrophobic aromatic moiety, these two compounds are solubilized more readily in micellar phase and that may cause pronounced effect on the acid-base equilibrium. Moreover, investigations of ground and excited state proton-transfer reactions in organized molecular assemblies (black bilayer membranes, vesicles, micelles monolayer aggregates etc.) are very important and provide unique information about the local structure and dynamics of such systems. These data are necessary to understand mechanism of the natural proton transport, which is of primary importance for bioenergetics and some other biological processes, and to design model and artificial systems for solar energy conversion etc. Perhaps the most widely studied excited state is the ionization of aromatic hydroxy compounds; and among them naphthols are most important molecules, which are appropriate for studies in micellar and vesicular solutions. Therefore, the effect of interfacial polarity on the acid-base equilibrium of naphthols in the ground state is very interesting aspect for investigation.

The primary objective of the present study is, therefore, to obtain a quantitative assessment of the factors, which are responsible for the difference between the apparent acid-base equilibrium constant of an interfacially located pH indicator molecule and its bulk aqueous pK_a value (pK_a^w). More specifically, following four points have been considered during the acid-base equilibrium study of indicator (probe) molecules in the present work.

(i) Variations of pK_a's, which appear in the study of an interfacial acid-base equilibrium, are characterized.

(ii) Titration of all indicators (molecular probe) in charged and uncharged micelles is described.

(iii) The observable shifts of "apparent" pK_a which is partitioned explicitly into a component due to the electrical potential and a

component caused by a change of polarity for a charged micelle is described.

(iv) By comparing the shift of the interfacial intrinsic pK_a^i to the pK_a shift measured in non-polar non-aqueous solvents, an attempt has been made to estimate the effective interfacial dielectric constant wherever possible, exhibiting the indicators as probes of interfacial polarity in same systems.

The pK_a values of OH groups of the present indicator molecules in aqueous medium are listed below:

TABLE: 2

Indicator Molecules	**Abbreviation used**	**pK_a^w**
5(OH) indole	HIn	11.04
5(OH)-L-Tryptophan	HTr	11.15
L-Tyrosine	Ty	10.05
L-Tyrosinemethylester	TyE	11.09
1-Naphthol	1 Nph	9.39
2-Naphthol	2 Nph	9.50

The acid-base equilibrium of the above indicator molecules is far more complex than that of a simple weak acid. As is apparent from the structures of

the molecules, several species could be postulated to be involved in the acid-base equilibrium.

However, one very important point worth mentioning is that ultraviolet spectra of all the above indicator molecules are influenced only on dissociation of hydroxy group attached to the aromatic ring. Therefore, acid-base equilibrium is monitored by the change of the ultraviolet spectra (figs. 3-20) by changing the solution pH. This gives rise to the required thermodynamic parameters.

3.2. Experimental

The indicator compounds applied for the present study, viz., L-Tyrosine was obtained from Himedia, India, L-Tyrosinemethylester, 5-Hydroxyindole, 5-Hydroxy-L-tryptophan were all Fluka products (USA) and were used as received. 1-Naphthol and 2-Naphthol were E. Merck, India products and were purified by vacuum sublimation (twice). The surfactants Cetyltrimethylammonium bromide (CTAB), Sodium dodecyl sulphate (SDS), Tween-40, Aerosol-OT (AOT) and Brij-35 were purchased from either Fluka, USA or Sigma Aldrich Chemical Co. USA and were used as received. 1,4-Dioxane (E. Merck, Germany) was further purified by distillation as mentioned in the literature.[80]

Stock solutions of the order of 10^{-3}M of all the pH indicators were prepared in pure water. The sample solutions of desired compositions of 1,4-dioxane-water mixtures and surfactant solutions were prepared from the stock solution with the help of micropipette. The pH of the solution was adjusted by adding small amount of dilute HCl or NaOH solutions and was measured with pH meter (model-Systronics:361, India). The uv spectra were recorded on a Shimadzu Spectrophotometer (model-UV 240, Japan). All the measurements were carried out at 298$\pm$1 K.

In pure water and aqueous micellar solutions, the negative logarithm of the hydrogen ion activity was taken as equal to the pH meter reading. However, for the organic solvent-water mixtures, the pH meter reading is not a direct measure of the negative logarithm of the hydrogen ion activity.[83] Van Uitert and Haas have shown that an empirical calibration can be made so that the pH meter reading can be converted into the stoichiometric hydrogen ion concentration.[81] The equation they derived for 1,4-dioxane-water mixtures was

$$-\log[H^+] = B + \log U_H^0 + \log \gamma_{\pm}^m \qquad (16)$$

where B is the pH-meter reading and $\log U_H^0$ is a correction factor which is independent of ionic strength and is attributable to two effects[81]: (i) the liquid junction potential being a function of the solvent composition, and (ii) the medium effect on the activity co-efficient of the hydrogen ion varying with solvent composition. $\gamma_{\pm}^m$ in equation (16), the mean ionic activity co-efficient for hydrochloric acid, referred to the particular 1,4-dioxane-water mixture at infinite dilution. The values for $\gamma_{\pm}^m$ can be obtained by interpolation of the values given by Harned and Owen[82] and taken in the present study from Drummond's work (Fig.1).[83]

The method generally applied to obtain the correction factor, $\log U_H^0$, was based on the dilution method, which has been described by Sanchez-Ruiz et al[84] and adopted by Drummond and co-workers.[83] The experimental procedure involves taking a 100% aqueous solution of known volume and hydrogen ion concentration and successively diluting this solution with known volumes of 1,4-dioxane. After each dilution and a sufficient time delay to allow for equilibration, the pH-meter reading B, is taken. The values of $\log U_H^0$ for each of the various 1,4-dioxane-water mixtures are then calculated on the basis of equation (16), and the tabulated $\gamma_{\pm}^m$ values. For the 100% aqueous solution – $\log [H^+]$ is assumed to be equal to the quantity $[pH - \log(1/ \gamma_{\pm}^m)]$. For each successive 1,4-dioxane-water mixture, the stoichiometric hydrogen ion

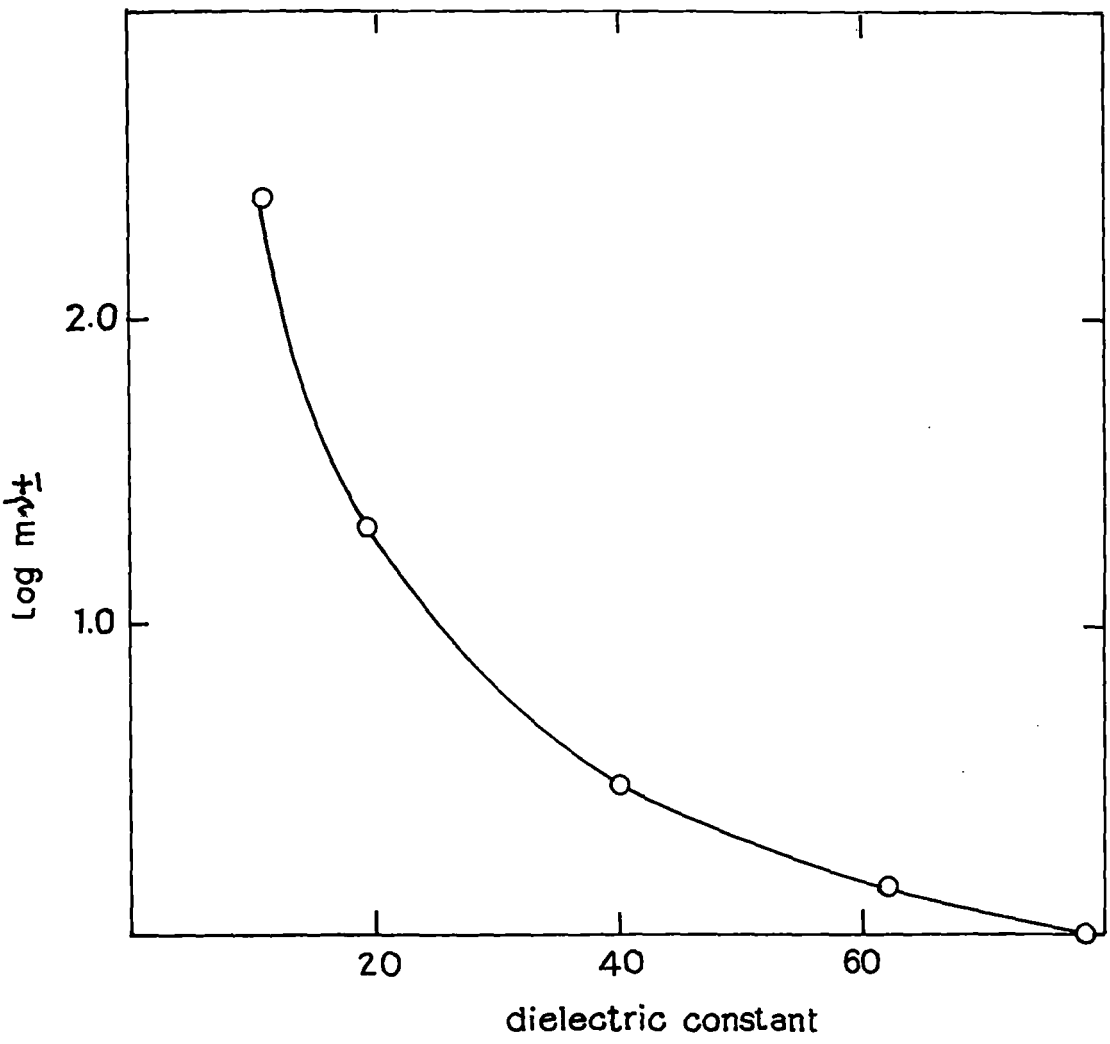

Fig. 1. log $_{m}\gamma_{\pm}$ values as a function of dielectric constant of 1,4-dioxane-water mixtures.

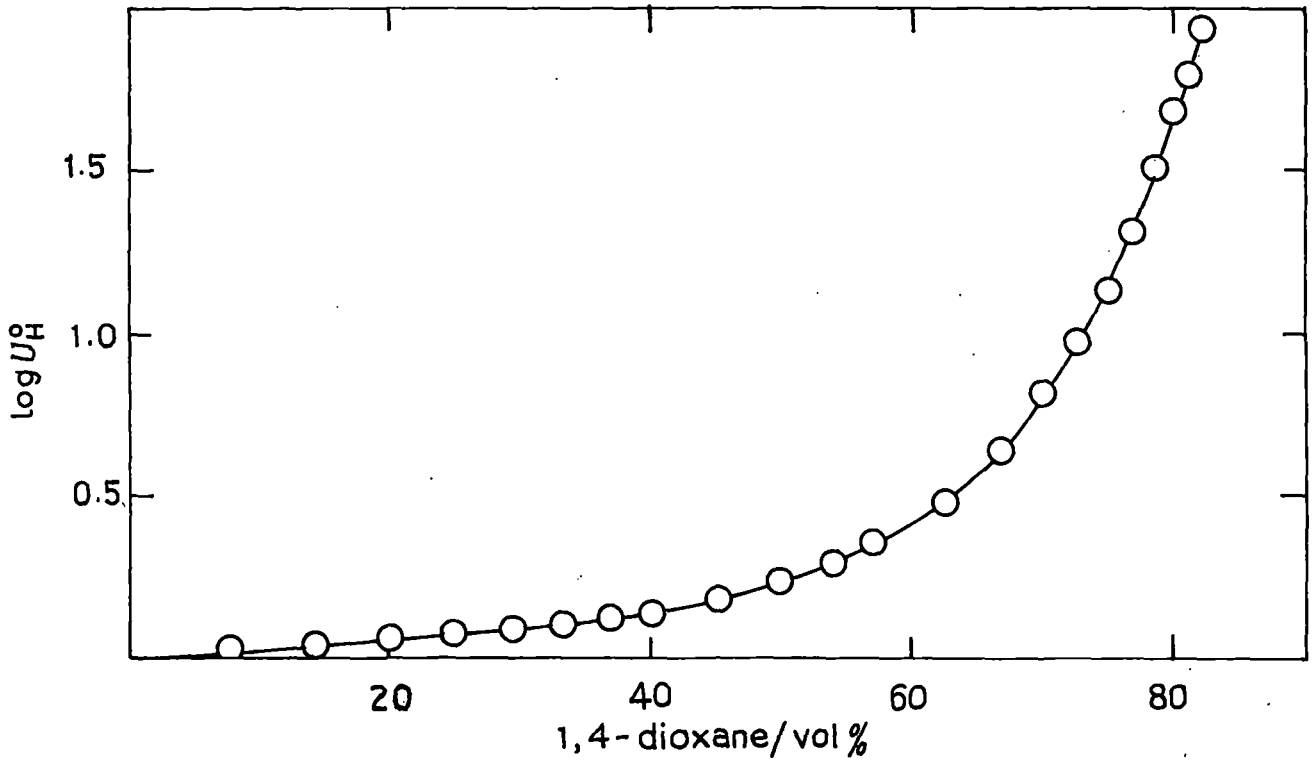

Fig. 2. The pH-meter correction factor, $\log U^0_H$, as a function of volume% 1,4-dioxane-water mixtures.

concentration is calculated by taking the dilution and the density of the solution into account. As no extra electrolyte is added to the solutions, the ionic strength is considered to be equal to the stoichiometric hydrogen ion concentration and the $\gamma_{\pm}^{m}$ values are calculated accordingly.

In figure 2, (adopted from ref.83), the values obtained for log U_H^0 are plotted as a function of the volume % of 1,4-dioxane in the 1,4-dioxane-water mixture.

When determining the various pK_a values, it may be assumed that the acid-base equilibrium of the present indicator molecules could be described by

$$HIN \overset{K_a}{\rightleftharpoons} H^+ + IN^- \text{ (Equation 7, with simplified notations)} \quad (17)$$

where HIN, IN, H^+ denote the protonated (acid), deprotonated (base) forms of the solute organic molecule and the proton respectively.

For the organic indicators in aqueous micellar solution, the apparent pK_a values were obtained from the change in the ultraviolet absorption spectrum of each indicator with bulk aqueous pH by means of the expression

$$pK_a^{obs} = pH - \log \frac{[IN]}{[HIN]} \quad (18)$$

with $$\frac{[IN]}{[HIN]} = \frac{\alpha}{1-\alpha} \quad (19)$$

and $$1-\alpha = \frac{A_{IN} - A}{A_{IN} - A_{HIN}}$$

where A represents the uv absorbance at the uv wave length band maximum of the deprotonated form of the indicator, λ_{max}, at a given pH, A_{HIN} the absorbance at λ_{max} when all the indicator molecules are protonated and A_{IN} the absorbance

at λ_{max} when all the indicator molecules are deprotonated. Representative ultraviolet absorption spectra for 5-Hydroxyindole, 5-Hydroxy-L-tryptophan, L-Tyrosine, L-Tyrosinemethylester, 1-Naphthol and 2-Naphthol, as a function of bulk aqueous pH are shown in figs. 3-20. Tables 3-7 gives the positions of the uv absorption band maximum of the indicator molecules in the media investigated.

The thermodynamic acid-base equilibrium constant for the reaction described by equation (17) in 1,4-dioxane-water mixtures is given by :

$$pK_a^m = B + \log U_H^o - \log \frac{[IN]}{[HIN]} - \log \frac{\gamma_{IN}^m}{\gamma_{HIN}^m} \qquad (20)$$

where γ_{IN}^m and γ_{HIN}^m denote the activity co-efficient of the base and acid forms of the indicators, respectively, referred to the particular 1, 4 dioxane-water mixture at infinite dilution. It is not completely clear how one should approximate the activity co-efficients of large complex organic ions such as the present indicator molecules. Consequently, the pK_a^m values given in this work neglect the activity co-efficient term.[83]

pH titrations in 1,4-dioxane-water mixtures were carried out with low indicator concentrations.(1.0×10^{-4}) mol dm^{-3}, and with no added electrolyte other than the HCl and NaOH required to perform the titrations. These HCl and NaOH additions were always kept to a minimum. The high pH and low pH spectra were always the final spectra to be taken in an experiment to determine a pK_a^m. At the background of low ionic strength, the interpolated magnitudes of the mean activity co-efficients of HCl in dioxane-water mixtures suggests that for the present composition of the mixtures, the activity co-efficient term in equation (20) is negligibly small. Hence the pK_a^m values of this work in the experimental mixtures are believed to approximate well the thermodynamic acid-base equilibrium constants.

3.3. Results and discussion

The theoretical background to the forthcoming analysis of the interfacial protonation-deprotonation equilibrium of the present indicator (probe) molecules has been given in pages 12 to 16 of the current chapter. Provided there is no significant contribution to the apparent acid-base equilibrium constant of an interfacially located organic molecules from specific solute-solvent interactions, the following relationship hold:

$$pK_a^i = pK_a^m - \log m\gamma_{H^+} \quad (21)$$

$$pK_a^0 = pK_a^i + \log \frac{\gamma_{IN}^i}{\gamma_{HIN}^i} \quad (22)$$

$$pK_a^0 = pK_a^{obs} + \frac{F\psi_0}{2.303RT} \quad (23)$$

where $m\gamma_{H^+}$ is the medium effect on the proton as discussed thoroughly by Drummond and co-workers.[83] γ_{IN}^i and γ_{HIN}^i denote the activity co-efficients of the deprotonated and protonated forms of the indicator molecules respectively, referred to the interfacial phase at infinite dilution, and F, R, T, Ψ_0 represent the Faraday constant, the universal gas constant, the absolute temperature and the electrostatic surface potential respectively. It may be recalled that while equation (21) describes equilibrium in 1,4-Dioxane-water medium, pK_a^i is related to pK_a^0 of the indicator molecule at the non-ionic micellar interface by the relation (22). However, the quantity log γ_{IN}/γ_{HIN} is negligibly small. Equation (23) is relevant for the acid-base equilibrium of the indicator molecule partitioned at the charged micellar interface.

In addition, it is convenient to define:

$$\Delta pK_a^m = pK_a^m - pK_a^w \quad (24)$$

$$\Delta pK_a^i = pK_a^i - pK_a^w \quad (25)$$

$$\Delta pK_a^0 = pK_a^0 - pK_a^w \qquad (26)$$

Figs 21 to 35 show the nature of variation of ΔpK_a^m and ΔpK_a^i as a function of the dielectric constant of 1,4 dioxane-water mixtures. The experimental data points refer to 0, 10, 20, 30, 50, 60 and 80 weight% of 1,4 dioxane in the mixtures. The dielectric constants were obtained from the work of Critchfield and co-workers[85]. As suggested by Drummond and co-workers,[83] the ΔpK_a^i values were derived from the ΔpK_a^m values with the aid of equation (21) above and by assuming that the $m\gamma_{H^+}$ can be approximated by the mean medium effect on HCl, $m\gamma_{\pm}$, in the same 1,4 dioxane in the mixtures. In calculating pK_a^0 for charged micelles, surface potential ψ of CTAB, SDS and AOT micelles were taken as +141 mv, -140 mv and, -140 mv respectively.[34]

3.3.1. Ultraviolet absorption spectra of 5-Hydroxyindole and 5-Hydroxy-L-tryptophan:

The uv spectra of 5-Hydroxyindole and 5-Hydroxy-L-tryptophan, as a function of the bulk aqueous pH in pure water as well as in different concentrations of cationic, anionic and non-ionic micellar solutions are shown in (figs. 3 to 20).

The spectral profile of 5-Hydroxyindole as a function of the bulk aqueous pH in pure in water is given in fig. 3. The spectral profile of the same probe in 0.02M CTAB (Fig.7), is representative of that obtained in 0.001M, 0.01M, 0.02M, 0.05M and 0.1M CTAB. Similarly, the spectral profile of 5-Hydroxyindole in 0.05M SDS solution (fig.8) is representative of those obtained in 0.001M, 0.01M, 0.02M, 0.05M and 0.1M of SDS. Similar spectra obtained for Tween-40 and Brij-35. The representative spectra of the above indicator molecule in Brij-35 is shown in fig. 9. The position of absorption band maximum λ_{max} for protonated and deprotonated forms of 5-

Hydroxyindole in each of the media investigated are given in table 3. The spectra exhibit a sharp isobestic point indicating the presence of an well defined protonation-deprotonation equilibrium.

Figs. 3-20 show the ultraviolet absorption spectrum of 5-Hydroxy-L-tryptophan as a function of the bulk aqueous pH in pure water and in different representative concentrations of CTAB, SDS, Tween-40, and Brij-35.

Since the molecular structure of 5-Hydroxyindole and that of 5-Hydroxy-L-tryptophan are similar, their uv spectral profile are also similar. Table-1 contains the λ_{max} values for the protonated and deprotonated forms of 5-Hydroxy-L-tryptophan in different media studied. These spectra also exhibit a sharp isobestic point.

As shown in figures 3 and 7-9 and as reported in table 3, micellar solubilization causes the λ_{max} of the protonated form of 5-Hydroxyindole to undergo a small blue shift in Tween-40 and dioxane-water mixtures. This can be ascribed to the effect that the different solvent properties of the micellar interfacial microenvironment has on energy of the π-π^* electronic transition. On the other hand, for the deprotonated form of 5-Hydroxyindole, λ_{max} is slightly red shifted in dioxane-water mixtures and SDS micelles while blue shift is observed in AOT micelles. In the case of 5-Hydroxy-L-tryptophan, as shown in figs 4, 10, 11, and as reported in table 4, the micellar solubilization causes the λ_{max} of the protonated form of the solute to undergo a very small blue shift in dioxane-water mixtures and registers no major change in the charged or uncharged micelles. The deprotonated form is, however, only slightly red shifted in dioxane-water mixtures with low dielectric constant and remain virtually unchanged in micellar interfaces. This indicates that there is little or no difference between the influence of the pure water and that of the micellar interfacial microenvironment on the energy of the π-π^* electronic transition.

Protonation-deprotonation equilibrium of OH groups of 5-Hydroxyindole and 5-Hydroxy-L-Tryptophan:

In 1,4 dioxane-water mixtures:

The pK_a^w values for protonation-deprotonation equilibrium of hydroxy groups of 5-Hydroxyindole and 5-Hydroxy-L-Tryptophan have been reported in tables 8 and 9. pK_a^m values for 5-Hydroxyindole and 5-Hydroxy-L-tryptophan as a function of 1,4-dioxane% in dioxane-water mixture as well as ΔpK_a^m a function of dielectric constants are shown in figures 21 to 23. Similarly, ΔpK_a^i values for 5-Hydroxyindole and 5-Hydroxy-L-tryptophan as a function of solvent dielectric constant in water-organic mixtures are shown in figures 24-26. pK_a^{obs} is found to vary from 11.041 to 16.213 for 5-Hydroxyindole for the variation of solvent composition from water to 80% dioxane in dioxane-water mixtures. Similarly, for 5-Hydroxy-L-tryptophan, a variation from 11.145 to 15.630 in pK_a^{obs} is registered.

In Micellar solutions:

The pH titration results for 5-Hydroxyindole and 5-Hydroxy-L-tryptophan in the aqueous micellar solutions investigated are summarized in tables 8 and 9 Also included in tables 18 and 19 are estimates of the effective interfacial dielectric constants, D_{eff} of the micelles for some systems. It is, however, possible to estimate the D_{eff} values if both of the protonated and deprotonated forms of the indicators have partitioned quantitatively into the interfacial micellar phase and if the micellar acid-base equilibrium are not influenced by specific molecular interactions or interfacial "salt effects".

It has been assumed that there is no contribution to pK_a^0 values due to the specific molecular interactions. Thus, by comparing a ΔpK_a^0 value with the plot of reference ΔpK_a^i values as a function of the solvent dielectric constant (Fig. 21-35), one can estimate the effective dielectric constant of the interfacial microenvironment of micelles. As the ΔpK_a^i values of the indicator molecules respond uniquely to changes in the solvent dielectric constant, these molecules

can provide unambiguous estimates of the interfacial D_{eff} at their average site of residence. For complex organic molecules, there will obviously be some ambiguity associated with the D_{eff} estimates.

For the charged micellar systems, the pK_a^0 values were determined from the known micellar surface potentials, the pK_a^{obs} values and equation (26), i.e.,

$$pK_a^{obs} = pK_a^{\circ} - \frac{F\psi}{2.303RT} \qquad (26)$$

The electrostatic surface potential of a CTAB micelle in the whole range of concentrations is considered to be +141 mV, whilst the surface potential of an SDS and AOT micelle are considered to be −140 mV in each case. Although, most of the indicator molecules applied in the present study are very little soluble in water, the possibility exists that the pK_a^{obs} value is a composite value comprising of the contributions from the species within the interfacial phase and the bulk aqueous phase. In this study, we attempted to avoid this occurrence by using high concentration of surfactants also. Nevertheless, the pK_a^{obs} results for Tween-40 and Brij-35 micelles suggest that a high percentage of the species in these systems may not have partitioned into the interfacial phase.

From table 8, it is observed that in the presence of non-ionic surfactant, viz., Tween-40 and Brij-35, pK_a^{obs} value is increased slightly compared to that in aqueous medium. This indicates that the deprotonated form of 5-Hydroxyindole is stabilized more in the non-ionic micellar media. On the other hand, in the presence of charged micelles, both CTAB and AOT micelles, pK_a^{obs} is decreased, indicating that the protonated form of the hydroxy derivative is stabilized. Like other surfactant micelles, SDS also registers a variation of pK_a values with concentration. At low concentration, (e.g., 0.01 M SDS) the pK_a^{obs} is smaller than that in water, but at higher concentrations, it gives larger values.

Protonation-deprotonation equilibrium of 5-Hydroxy-L-tryptophan also shows similar behaviour in micellar environment. This is not unexpected because of their structural similarities. The pK_a values are found to decrease significantly in CTAB and AOT micelles indicating stabilization of the deprotonated species. However, the changes in the pK_a^{obs} values are not very high but register an increasing trend in SDS and Brij-35 micelles. The negative ΔpK_a^0 values for SDS and AOT micelles are indicative of the fact that there are some specific interactions between the negatively charged head groups and the deprotonated anions of either 5-Hydroxyindole or 5-Hydroxy-L-tryptophan because ΔpK_a^i and ΔpK_a^m values for these indicator molecules are positive for organic-water media (Fig. 21 to 35).

On the other hand, the ΔpK_a^0 values of these indicators in Tween-40 and Brij-35 micelles are small. This indicates that the indicator molecules are not partitioned in non-ionic micellar interfaces efficiently. Although Fernandez and Formherz[34] using 4-Heptadecyl-7-hydroxy coumarin and 4-Octacycloxy-1-naphthoic acid as acid-base indicator, have shown that D_{eff} of ionic micelles can be equated to the D_{eff} of the interface of non-ionic micelles of surfactants with poly (ethylene oxide) head group, Drummond and co-workers[83] were of the opinion that this assumption is not valid in many cases and pK_a^{obs} value of weak acid-base equilibrium in ionic micelles can be explained on the basis of factors like low interfacial polarity, salt effect and specific interaction of the indicator species with the head groups of the surfactants. In the present study, the D_{eff} values determined for CTAB micellar interface by comparing the ΔpK_a^0 values with those of ΔpK_a^i values, shows that the effective dielectric constant varies from 38.8 to 52.2 yielding an average value of 43.1, while previous authors found a value of ~32 for interfacial polarity of CTAB micelle.[34] Further, observed variation of D_{eff} with CTAB concentrations indicates that the solubilization sites are different and depends on molar ratio of CTAB and the indicator. A locally varying dielectric constant as a function of distance from the charged surface of polyelectrolytes on lipid membranes has

been interpreted in many cases to justify experimental low dielectric constant values. In other words, it seems apparent that not all the 5-Hydroxyindole molecules are partitioned in the interfacial region but some must have been accumulated at a distance from the surface of the micelle and the estimated D_{eff} gives an average value for such a distribution. Moreover, to justify the observed variation of D_{eff} with CTAB concentration it may be argued that the population of the indicator molecules in the interfacial and surrounding regions is redistributed as the molar ratio of indicator and CTAB changes. However, comparison of the results of ΔpK_a^0 (Table 14) and ΔpK_a^i (Figs. 21-35) for 5-Hydroxy-L-tryptophan molecule yield an average D_{eff} value for interfacial polarity of CTAB micelle as ~55. At high concentration of CTAB micelle (0.1M), the D_{eff} value is found to be 47.

3.3.2. Ultraviolet absorption spectral study of protonation-deprotonation equilibrium of L-Tyrosine and L-Tyrosinemethylester

As depicted in figs. 3-20, the spectral feature of L-Tyrosine and L-Tyrosinemethylester are more complicated than those of 5-Hydroxyindole and 5-Hydroxy-L-tryptophan. The protonation-deprotonation equilibrium of hydroxy groups in L-Tyrosine and L-Tyrosinemethylester influences the corresponding uv spectra to a great extent and in each case three clear and well defined isobestic points are exhibited. The uv absorption spectra of both L-Tyrosine and L-Tyrosinemethylester have become complicated due to the presence of three isobastic points in the wave length region 220 to 300 nm. However, the absorbance of the conjugate base of hydroxy groups of the indicators were accessible from the λ_{max} at ~240 nm. While L-Tyrosine is found to be well behaved pH indicator to study micellar interfacial microenvironment, L-Tyrosinemethylester has been selected to examine the effect of carboxyl anionic charge, if any, present in L-Tyrosine molecule.. The spectral profile of L-Tyrosine in 0.02M CTAB solution (fig. 15) is

representative of that obtained in 0.001M, 0.01M, 0.02M, 0.05M and 0.1M CTAB. Similarly, the spectral profile of L-Tyrosine in 0.02M SDS, 0.001M Tween-40 and 0.001 Brij-35 are representative of those observed in other concentrations. The position of ultraviolet absorption band maximum λ_{max}, for the protonated and deprotonated forms of L-Tyrosine in each of the media investigated are given in tables 5 and 6.

As shown in figures 12-15 and as reported in table 5, the micellar solubilization causes the λ_{max} of the protonated form of L-Tyrosine to undergo blue shift in dioxane-water mixtures as well as in the presence of micellar interfacial microenvironment. Maximum shift has, however, been observed in SDS micelles. This can again be ascribed to the effect that the different solvent properties of the micellar interfacial microenvironment has on the energy of the π-π^* electronic transition. In contrast to this, the λ_{max} values for the deprotonated form of L-Tyrosine, figs 12-15 and table 5, is found to undergo a red-shift in dioxane-water mixture of low dielectric constant. However, this red-shift in presence of micellar interfacial microenvironment is most prominent in AOT micelles but less prominent in SDS micelles. It is unlikely that interfacial microenvironment of SDS micelles being more "aqueous like" in nature for the deprotonated form of L-Tyrosine and less so in case of protonated L-Tyrosine. On the other hand, it may be attributed to the fact that due to the existence of an isoelectric point of L-Tyrosine near 5.66, the protonated form remains more close to the SDS micellar interface than those of deprotonated form due to electrostatic repulsion at high pH. However, hydrophobic interaction of the amino acid with AOT micelles seems to be greater resulting in the quite large red shift of λ_{max} of deprotonated L-Tyrosine in presence of AOT micelles. As shown in figs 16-18 and as reported in table 5, the effect of micellar interfacial microenvironment or the medium effect (in presence of dioxane-water mixtures) on λ_{max} values of protonated and deprotonated forms of L-Tyrosinemethylester is more or less same as that of L-Tyrosine and the result does not indicate any large effect of estarification of carboxylic acid group of L-Tyrosine. This indicates that the effect of anionic

charge or the existence of isoelectric point (there is no isoelectric point in TyE) are once again not the dominating factors and the overall complex and nearly identical structure of the molecules determine their resultant properties with respect to electronic transition. Tables 10-11 show that, in the presence of non-ionic micelles, viz., Tween-40 and Brij-35 micelles, pK_a^{obs} values of both L-Tyrosine and L-Tyrosinemethylester are increased compared to those in aqueous medium. This indicates that the deprotonated forms of both the indicator molecules are stabilized more in the non-ionic micellar media. On the other hand, mostly in charged micelles (e.g., CTAB and SDS), pK_a^{obs} values are decreased indicating that the protonated forms are stabilized in CTAB and SDS micelles. However, unlike the results of 5-Hydroxyindole and 5-Hydroxy-L-tryptophan, AOT micelle stabilizes mostly the deprotonated forms of L-Tyrosine and L-Tyrosinemethylester. ΔpK_a^0 values (Tables 10 and 11) for the present indicator once again yield values which are negative for SDS and AOT micelles. This discrepancy may once again be interpreted as the result of strong electrostatic interaction between the deprotonated phenoxide ion and the carboxylate anion with that of micellar anionic head groups.

Values of ΔpK_a^i and ΔpK_a^m for both of the indicators are consistently positive in 1,4-Dioxane-water mixtures (Tables 15 and 16). Effect of carboxylate anion in L-Tyrosine is not very apparent if one compares the result of L-Tyrosine with that of its methyl ester counterpart. For the present indicator molecules, ΔpK_a^0 values are small but positive for Tween-40 and Brij-35 micelles. This indicates that these indicators are not efficiently partitioned in the interfacial region of the non-ionic micelles. However, both L-Tyrosine and L-Tyrosinemethylester are partitioned to a greater extent in CTAB micelles yielding larger positive ΔpK_a^0 values which is consistent with the ΔpK_a^i and ΔpK_a^m values in the organic-aqueous medium (Tables 20-21). D_{eff} values have been estimated by comparing ΔpK_a^0 values of L-Tyrosine and L-Tyrosinemethylester in CTAB micelles with those of ΔpK_a^i for 1,4-Dioxane-water mixtures. The effective dielectric constant values for CTAB micellar interface for above two indicators are more or less same, i.e., 49 ± 1. This value

once again shows that the indicator molecules are distributed in the interfacial region of the micellar surface upto a certain distance.[86]

3.3.3. Ultraviolet absorption spectral study of protonation-deprotonation equilibrium of 1-Naphthol and 2-Naphthol

The spectral profiles of 1-Naphthol in different media under investigation are shown in figs. 19 and 20 The position of ultraviolet absorption band maximum λ_{max} for protonated and deprotonated forms of 1-Naphthol in each of the media investigated is given in table 7. As shown in figs. 19 and 20 and as reported in table 7, the micellar solubilization causes the λ_{max} of both the forms blue shifted to some extent except AOT. In AOT, the deprotonated form of 1-Naphthol is red shifted to a greater extent. All the spectra gives well defined conjugate acid and conjugate base absorption bands which allow one to determine the pK_a of acid-base equilibrium of the probe molecules in aqueous as well as interfacially located regions.

The ultraviolet spectra of 2-Naphthol is unfortunately quite insensitive to solution pH as is observed from its spectral profiles as a function of bulk pH. Therefore, no attempt has been made to determine the dissociation constant value of 2-Naphthol in aqueous or micellar media from ultraviolet spectroscopic measurement.

Considering the simpler aromatic structure and the high hydrophobic nature, 1-Naphthol may be thought to be a well-behaved probe molecule for protonation-deprotonation equilibrium study at micellar interface. However, the results obtained in case of 1-Naphthol was found to be comparable with those of other indicator molecules under investigation. These results also justify the use of these indicators as probe molecules. Table 12 shows that except in CTAB micelles, pK_a^{obs} values of 1-Naphthol are positive in all the anionic and non-ionic micelles. Therefore, it may be argued that the

deprotonated form of the indicator is stabilized in interfacial region of the micelles. However, in CTAB micelles at comparatively lower concentrations (0.001M to 0.02M), the deprotonated form is stabilized. The ΔpK_a^0 still give negative values in SDS and AOT micelles showing a repulsive interaction between the deprotonated forms of the Naphthol with the surfactant head groups. As a result, 1-Naphthol is not partitioned effectively in the micellar core in spite of its strong hydrophobic aromatic ring. In Tween-40 and Brij-35 micelles, the indicator molecules are partitioned more effectively than other four indicators as is evident from the high ΔpK_a^0 values (Table 12). The interfacial polarity of CTAB micelles (D_{eff}) determined by comparing ΔpK_a^0 values in the interface with that of ΔpK_a^i in 1,4-Dioxane-water mixtures (Table 12) shows that at high concentration of CTAB, 1-Naphthol is partitioned more efficiently and D_{eff} value of ~ 45 is obtained (Table 22). Like other indicator molecules studied in the present work, distribution of 1-Naphthol in the interfacial region of CTAB micelles, however, probably changes upto a limited distance as a function of CTAB concentration.

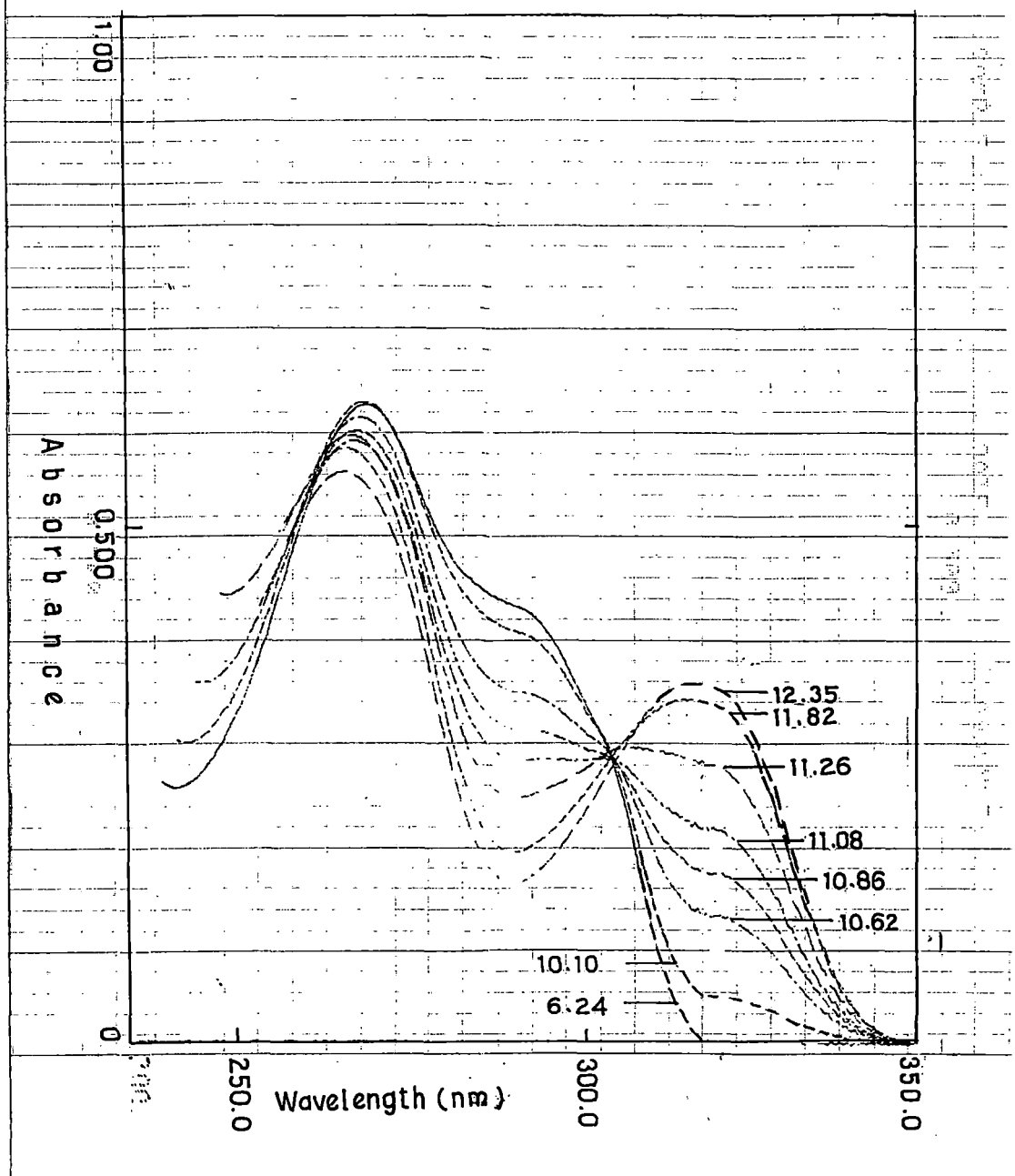

Fig. 3. Absorption spectrum of 5-Hydroxy indole ($1x10^{-4}M$) in water.

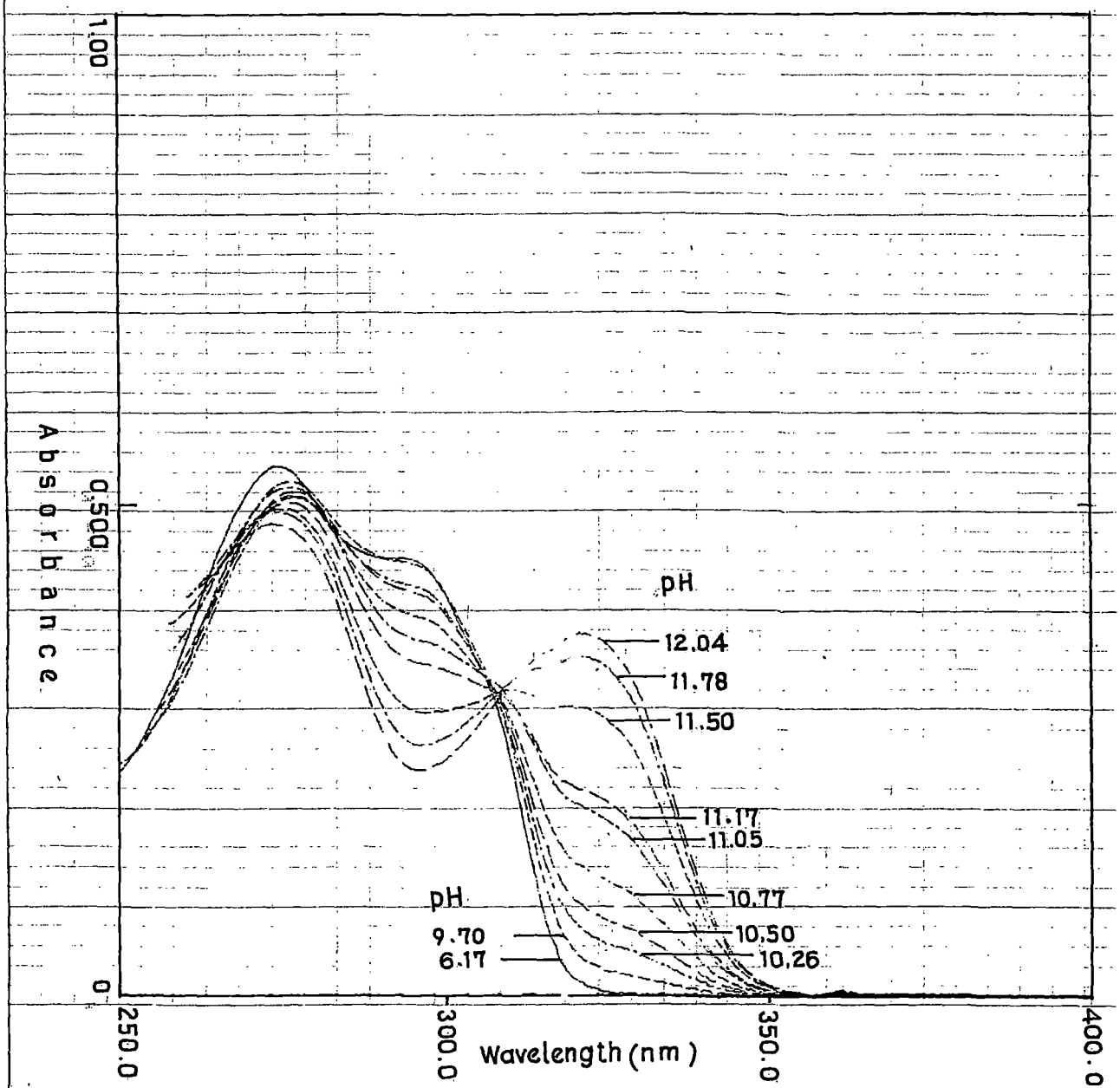

Fig. 4. Absorption spectrum of 5-Hydroxy-L-tryptophan ($1x10^{-4}M$) in water.

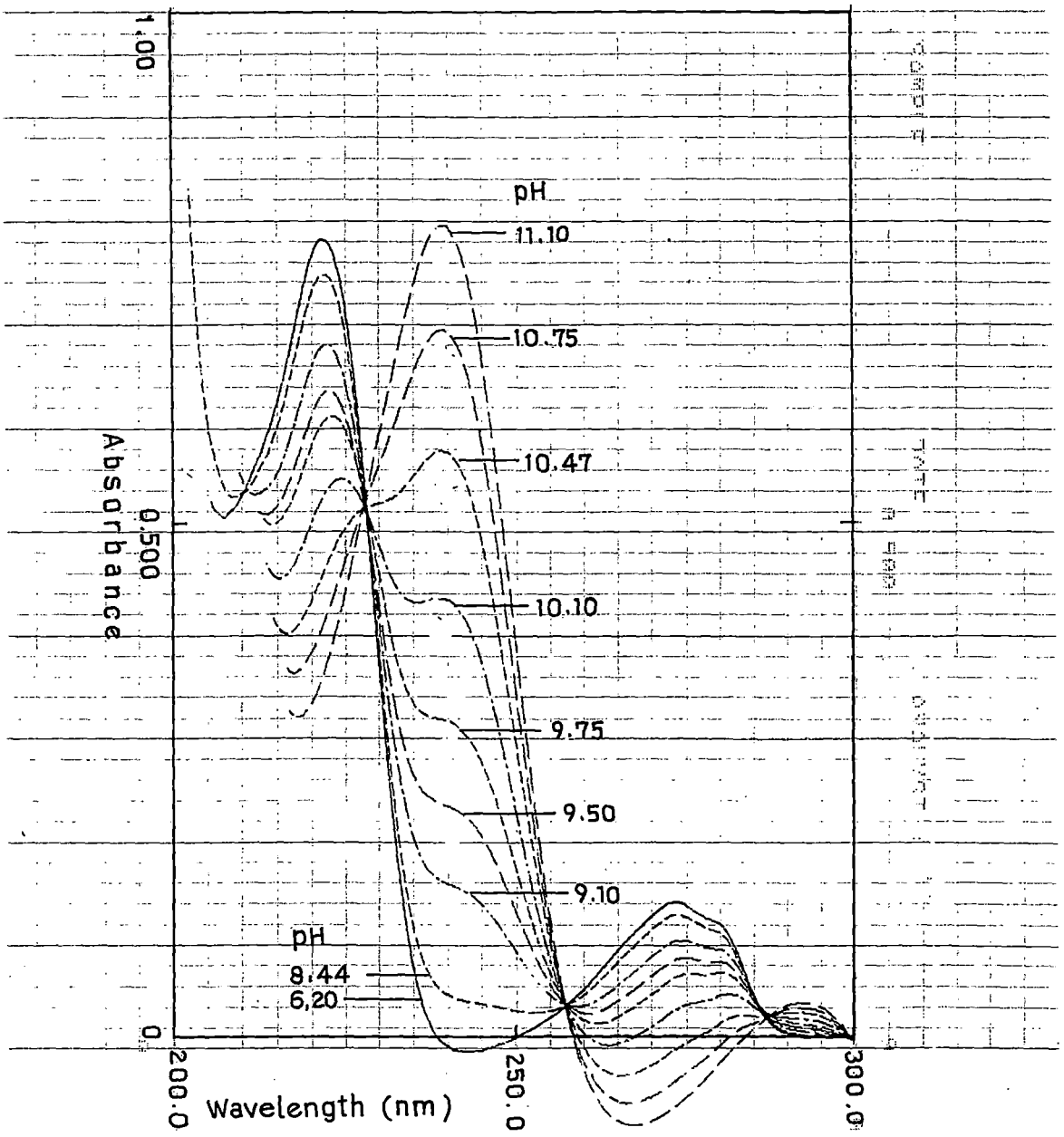

Fig. 5. Absorption spectrum of L-Tyrosine ($1x10^{-4}M$) in water.

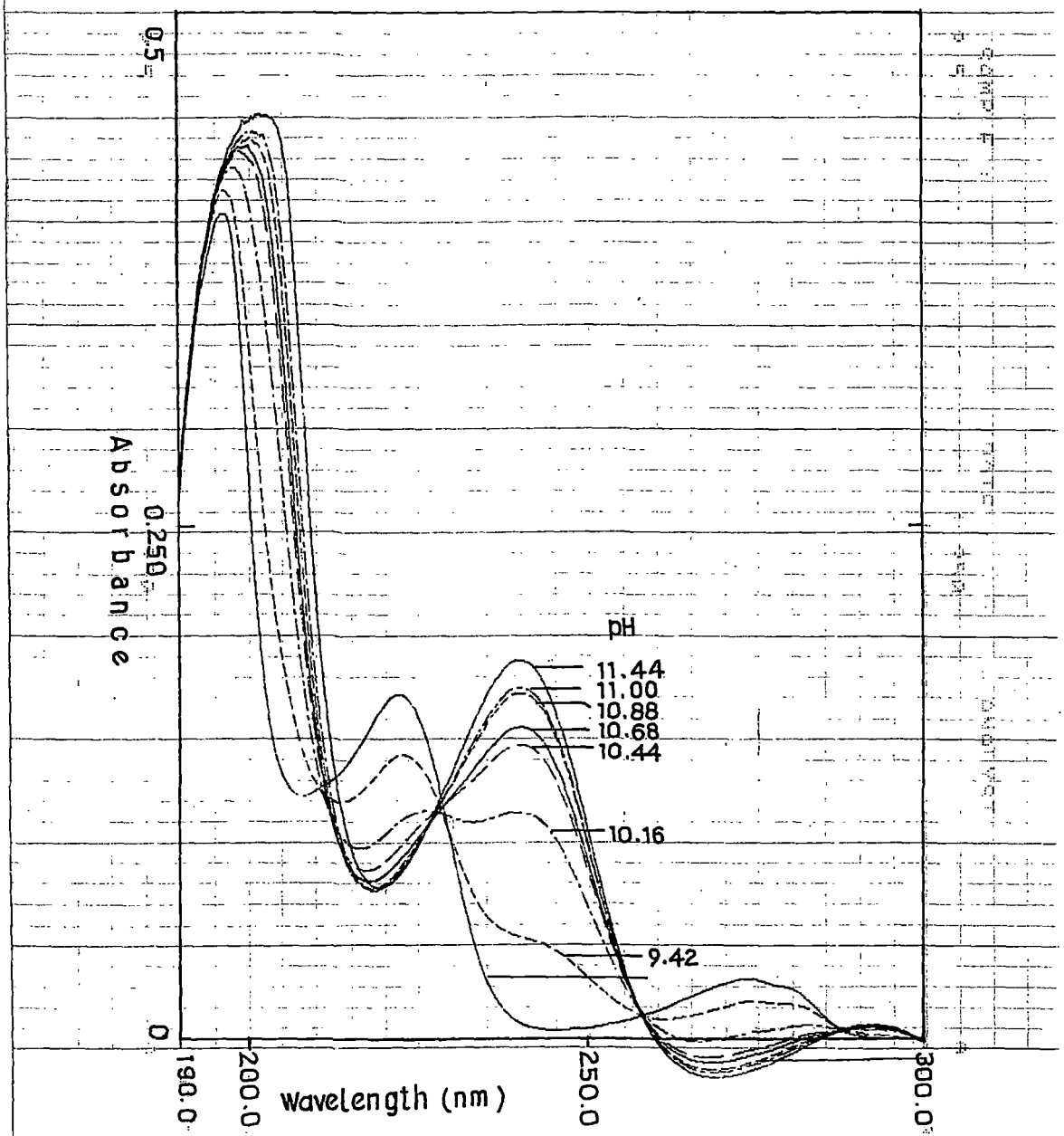

Fig. 6. Absorption spectrum of L-Tyrosine methyl ester(1×10^{-4}M) in water.

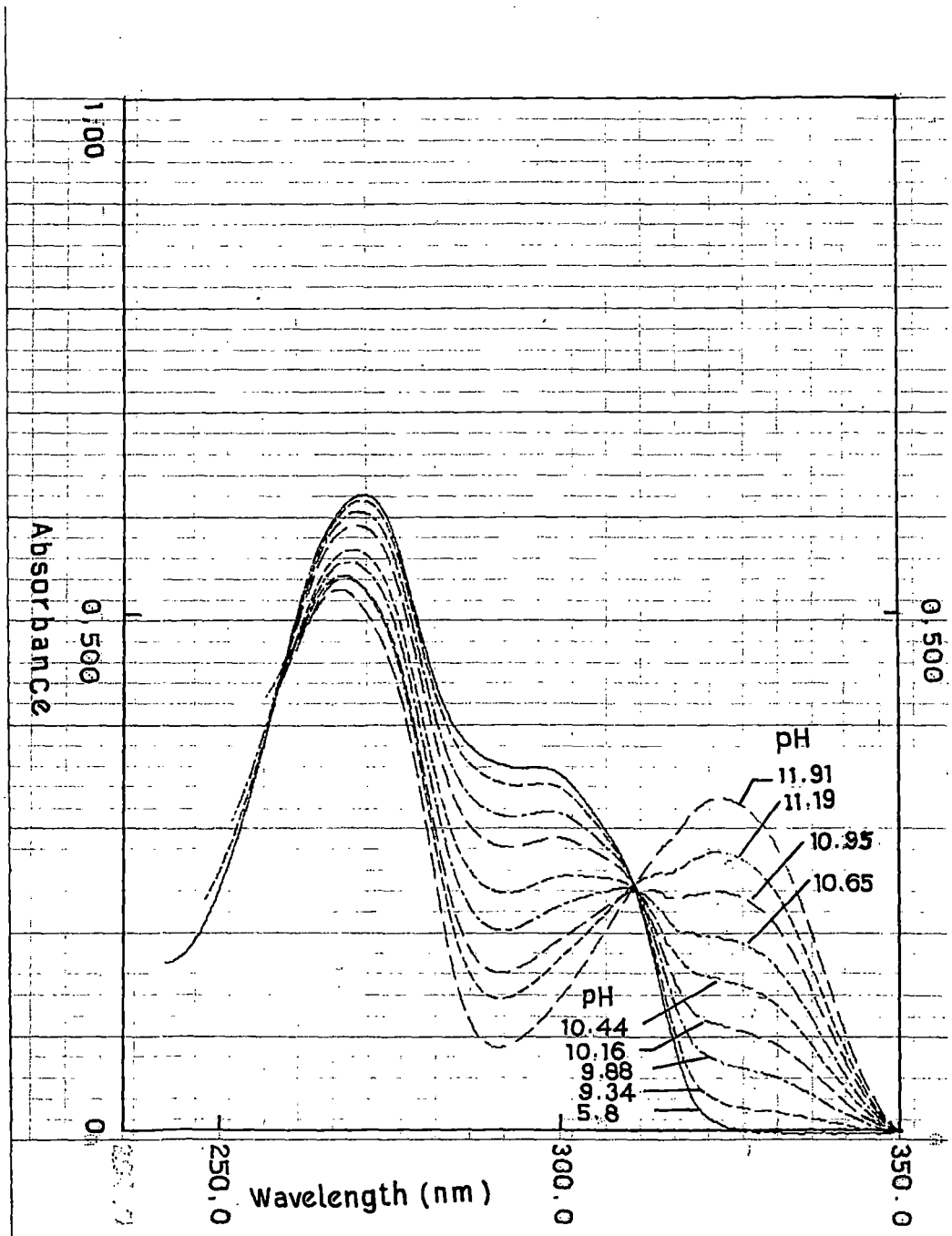

Fig.7. Absorption spectrum of 5-Hydroxy indole ($1x10^{-4}$M) in 0.02M CTAB solution.

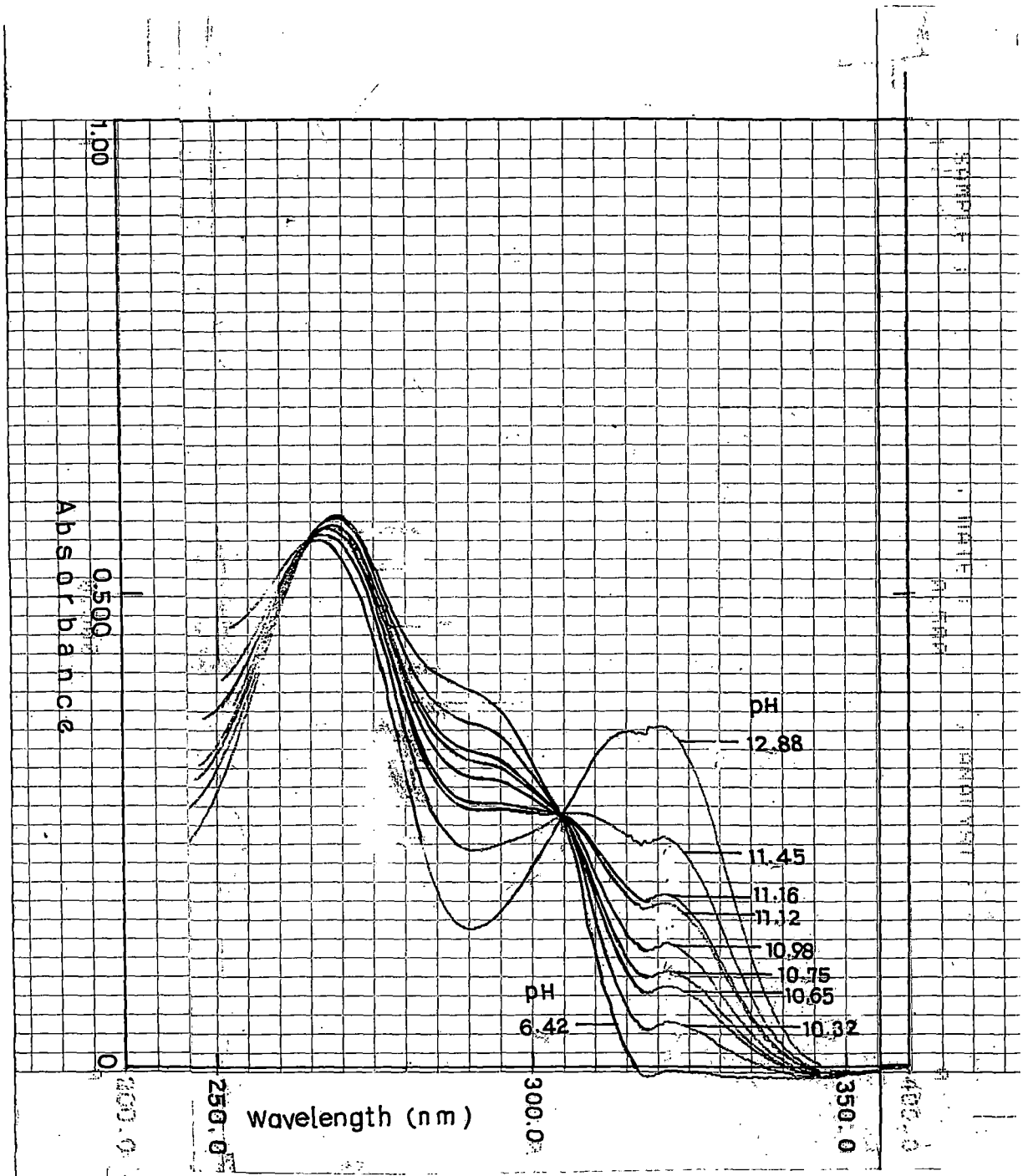

Fig. 8. Absorption spectrum of 5-Hydroxy indole ($1x10^{-4}$M) in 0.05M SDS solution.

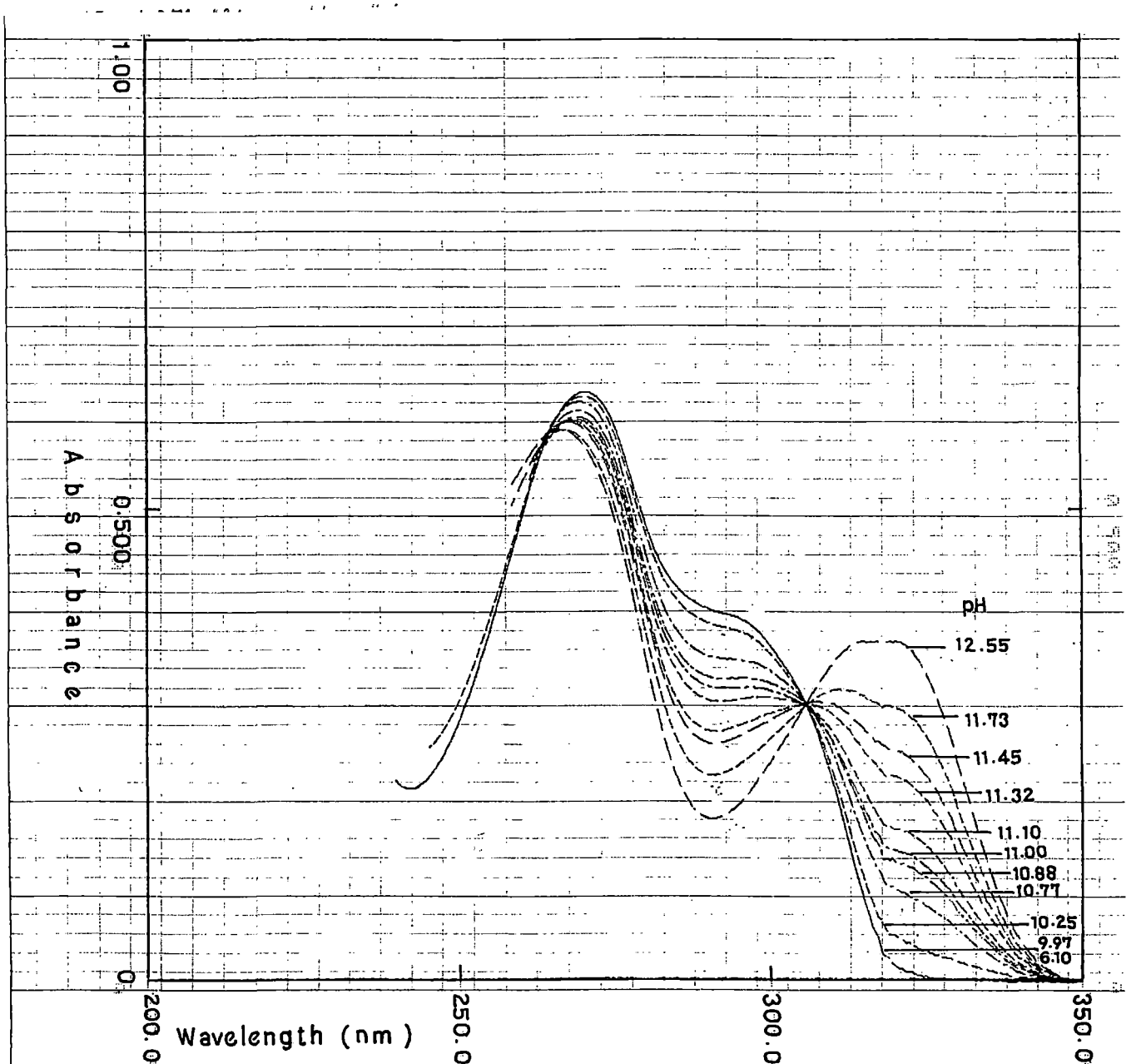

Fig. 9. Absorption spectrum of 5-Hydroxy indole ($1x10^{-4}$M) in 0.01M Brij-35 solution.

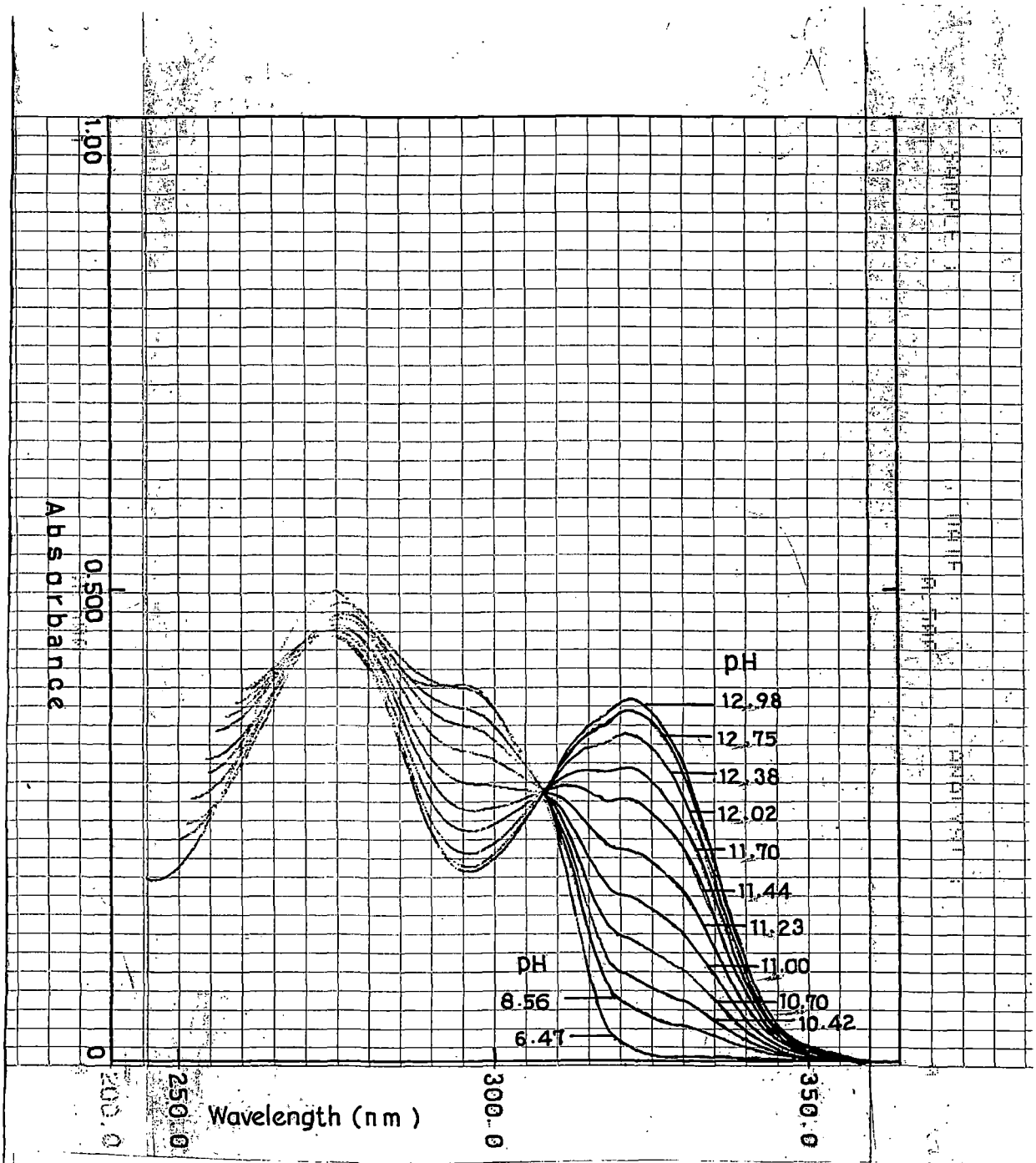

Fig.10. Absorption spectrum of 5-Hydroxy-L-tryptophan ($1x10^{-4}$M) in 0.1M SDS solution.

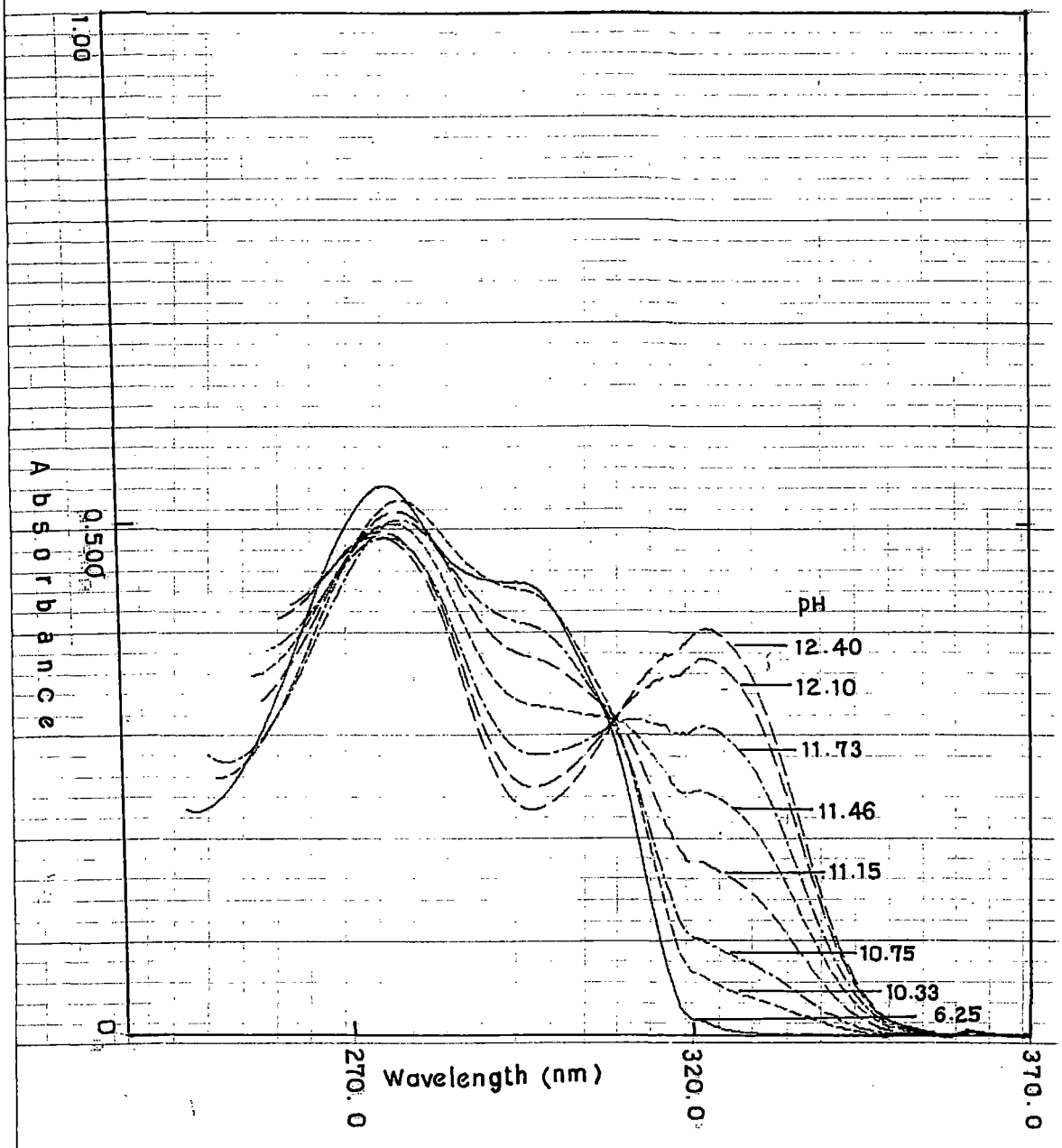

Fig. 11. Absorption spectrum of 5-Hydroxy-L-tryptophan ($1x10^{-4}$M) in 0.001M Brij-35 solution.

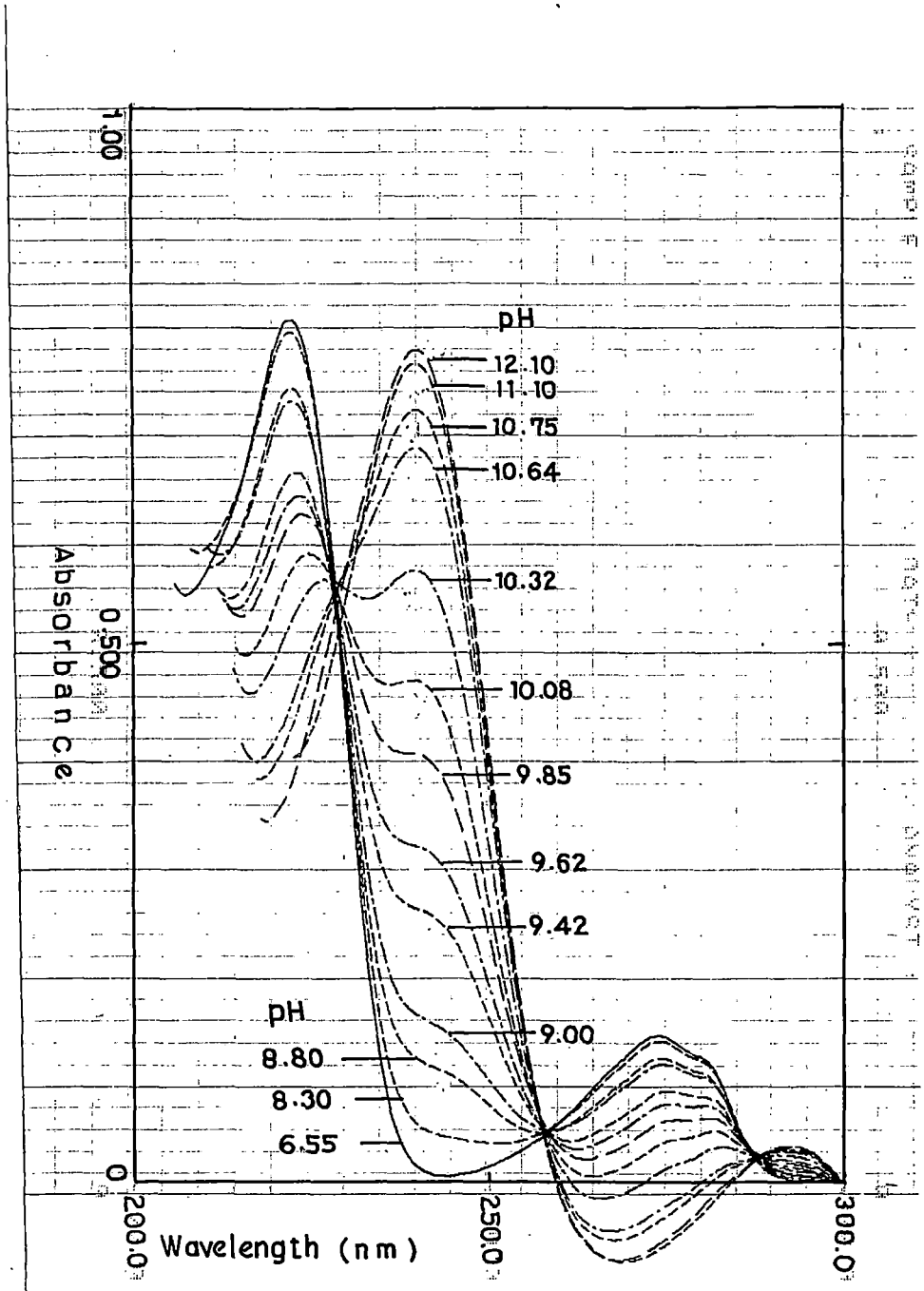

Fig.12. Absorption spectrum of L-Tyrosine ($1x10^{-4}$M) in 0.02M SDS solution.

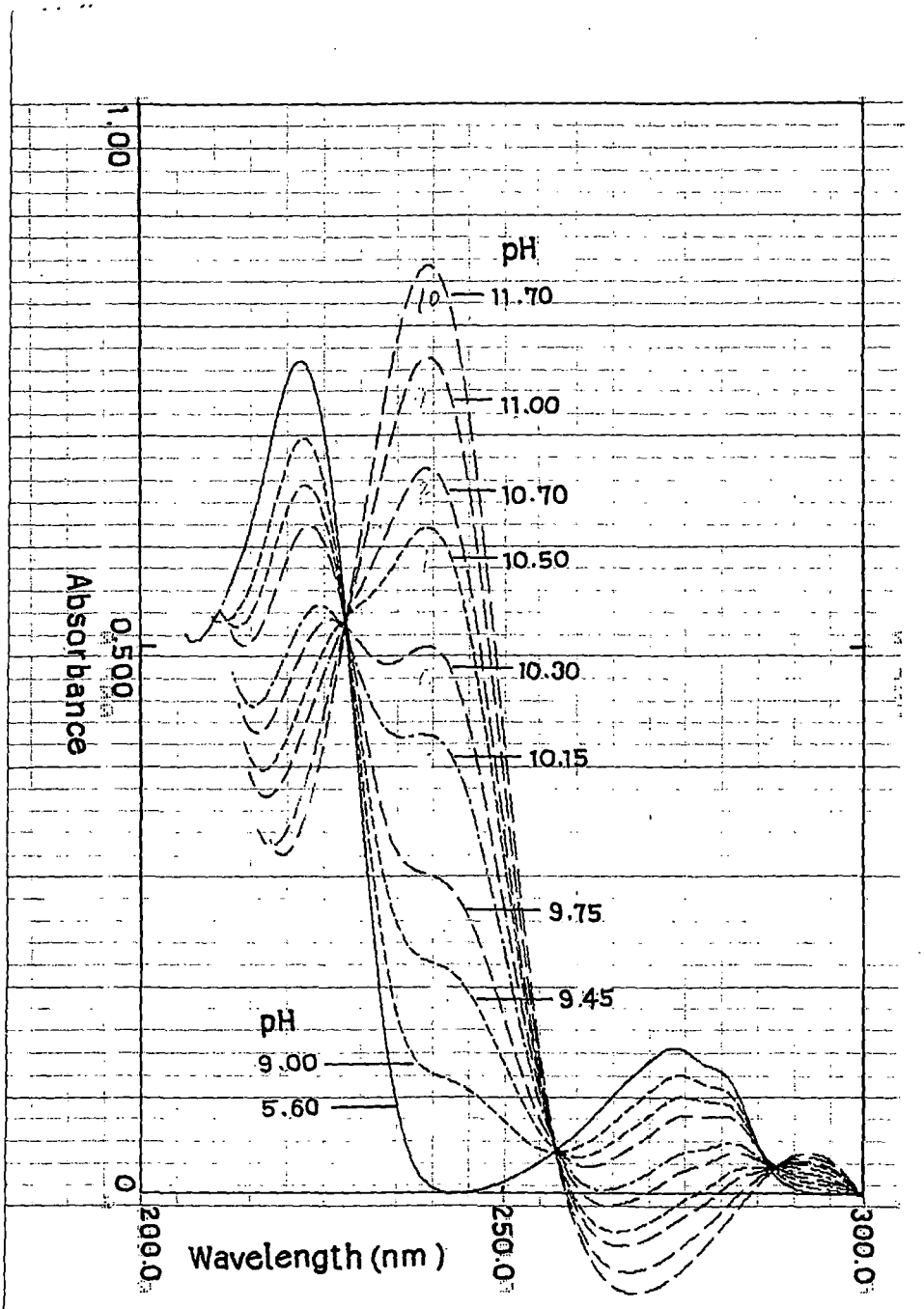

Fig. 13. Absorption spectrum of L-Tyrosine ($1x10^{-4}$M) in 0.001M Tween-40 solution.

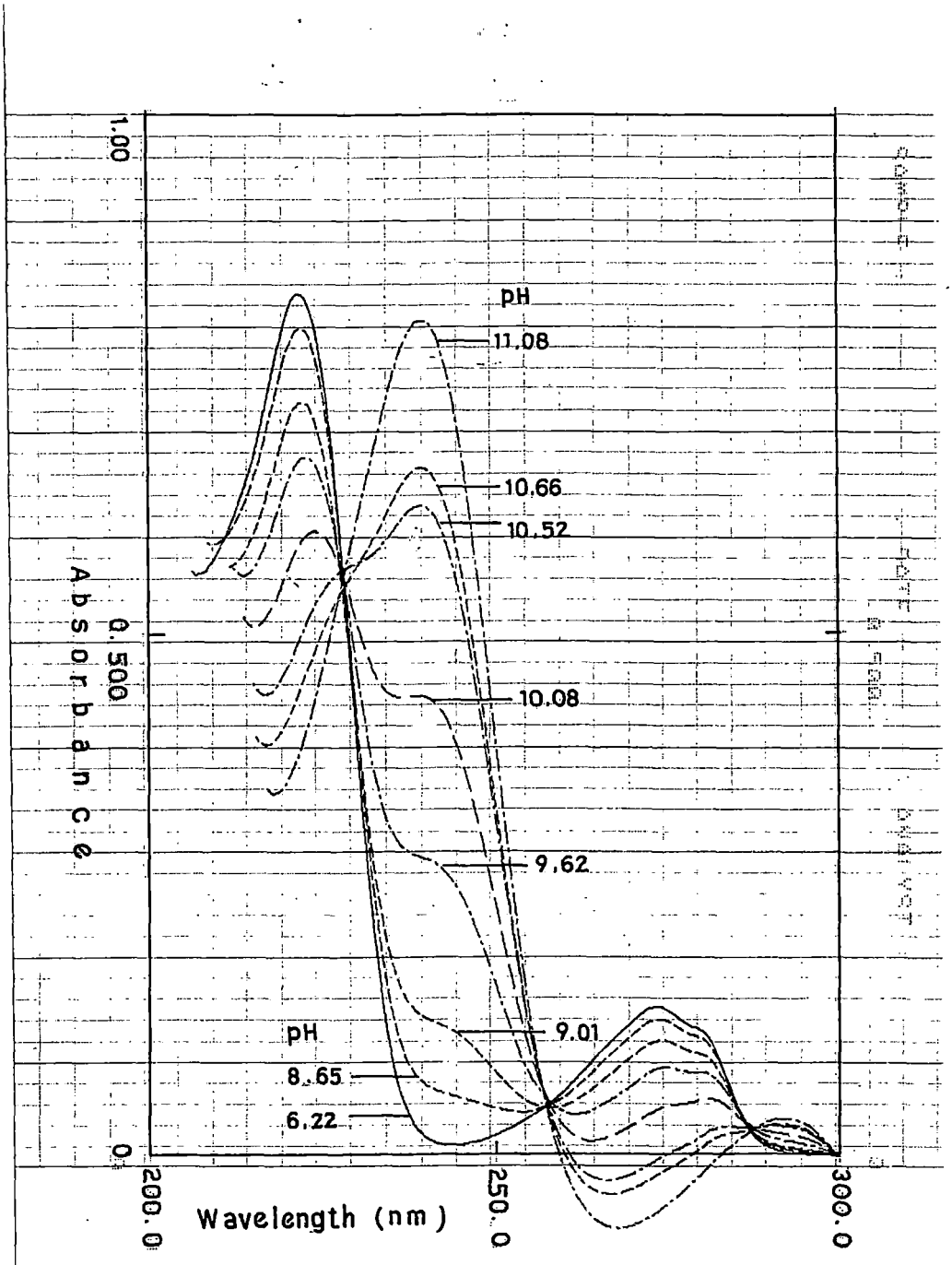

Fig. 14. Absorption spectrum of L-Tyrosine ($1x10^{-4}$M) in 0.001M Brij-35 solution.

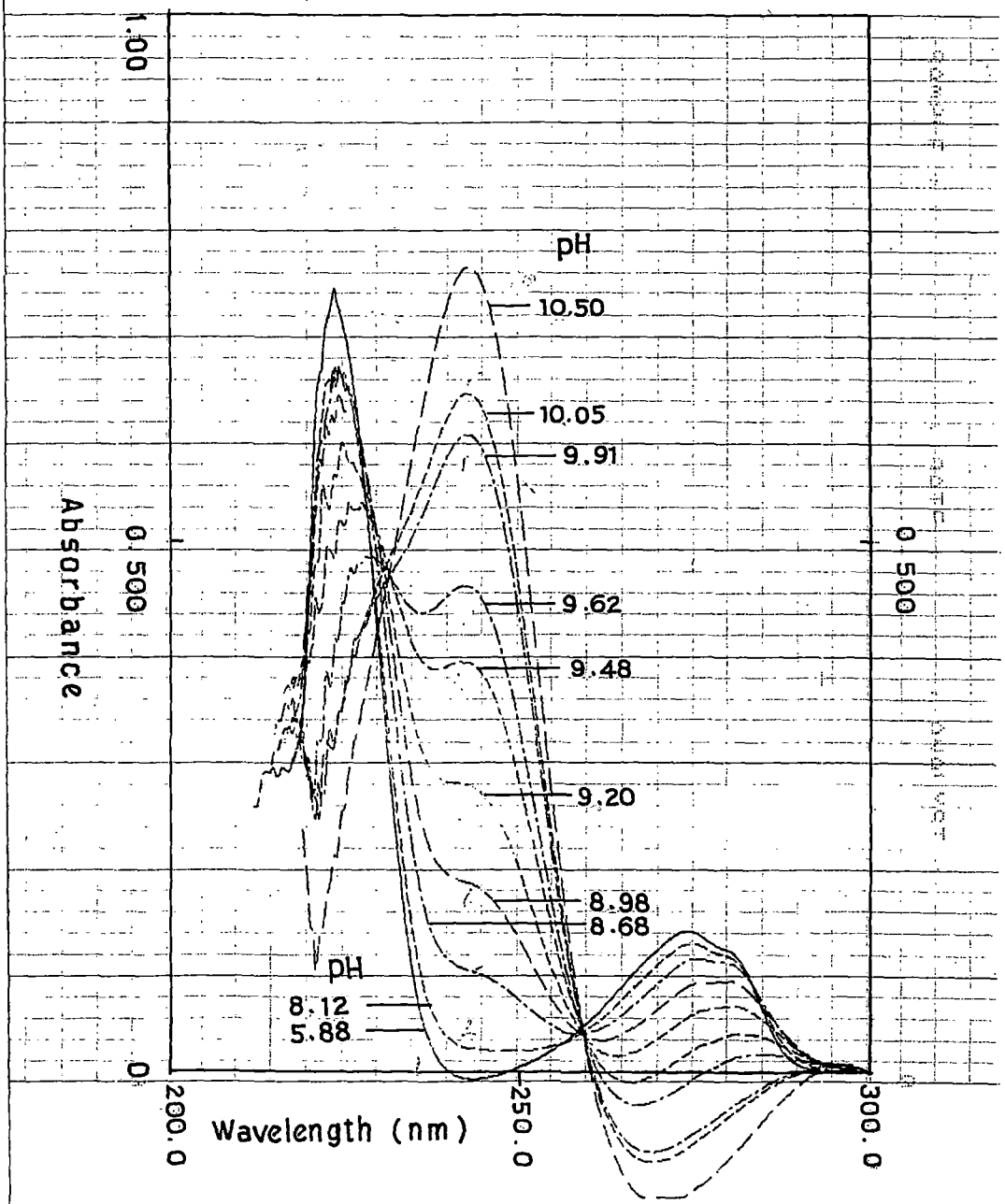

Fig. 15. Absorption spectrum of L-Tyrosine ($1x10^{-4}$M) in 0.02M CTAB solution.

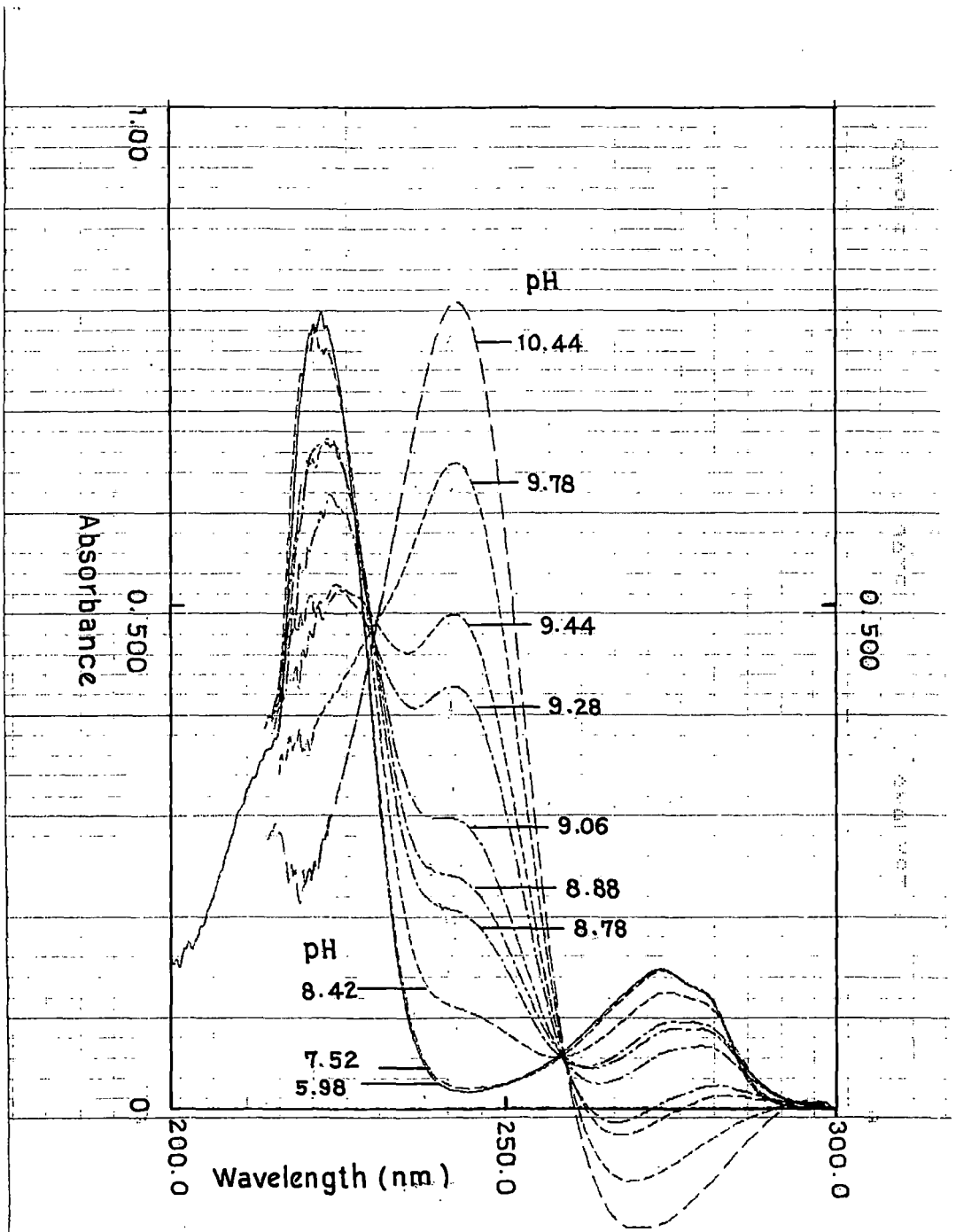

Fig. 16. Absorption spectrum of L-Tyrosine methyl ester ($1x10^{-4}$M) in 0.01M CTAB solution.

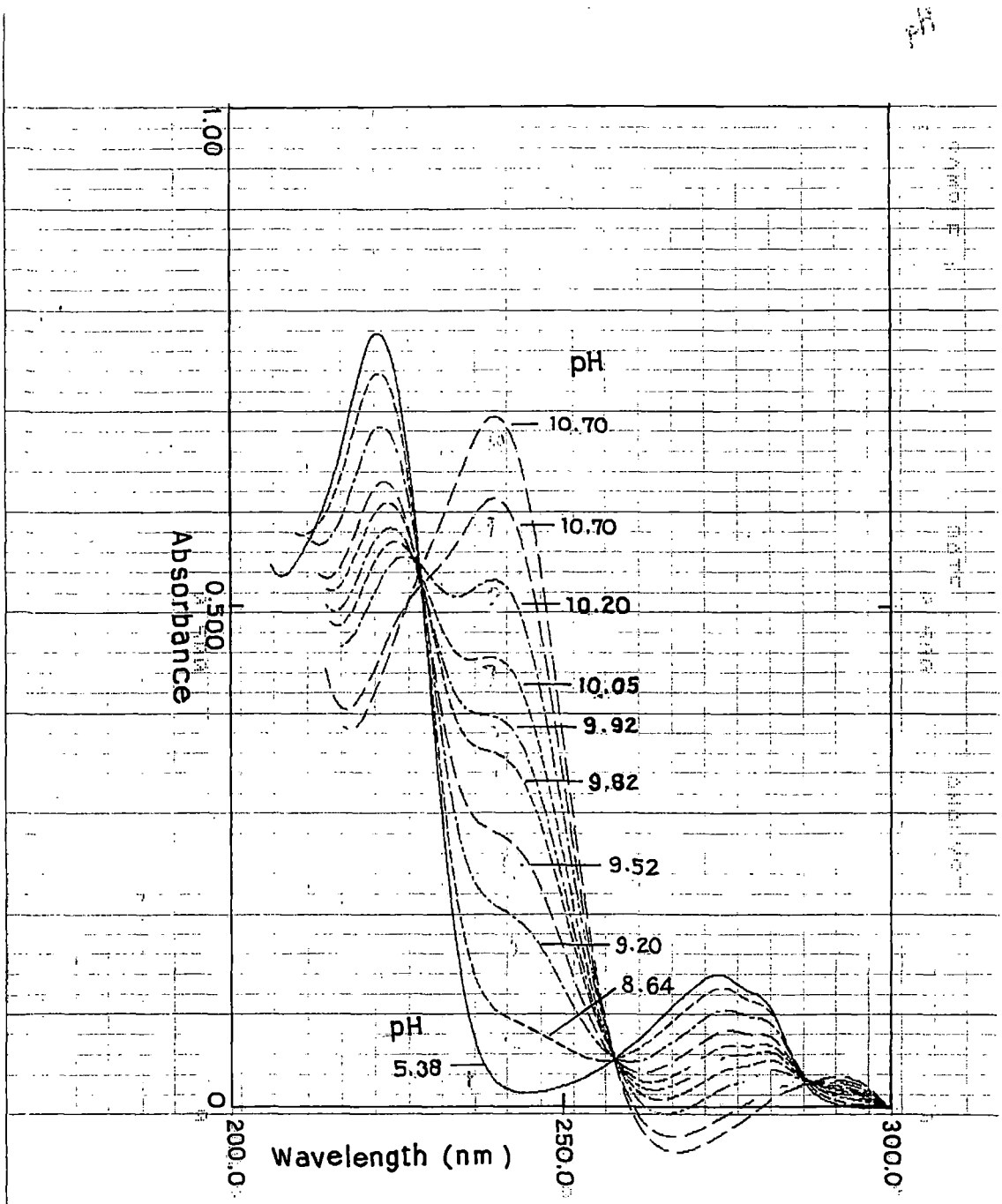

Fig. 17. Absorption spectrum of L-Tyrosine methyl ester ($1x10^{-4}$M) in 0.001M Tween-40 solution.

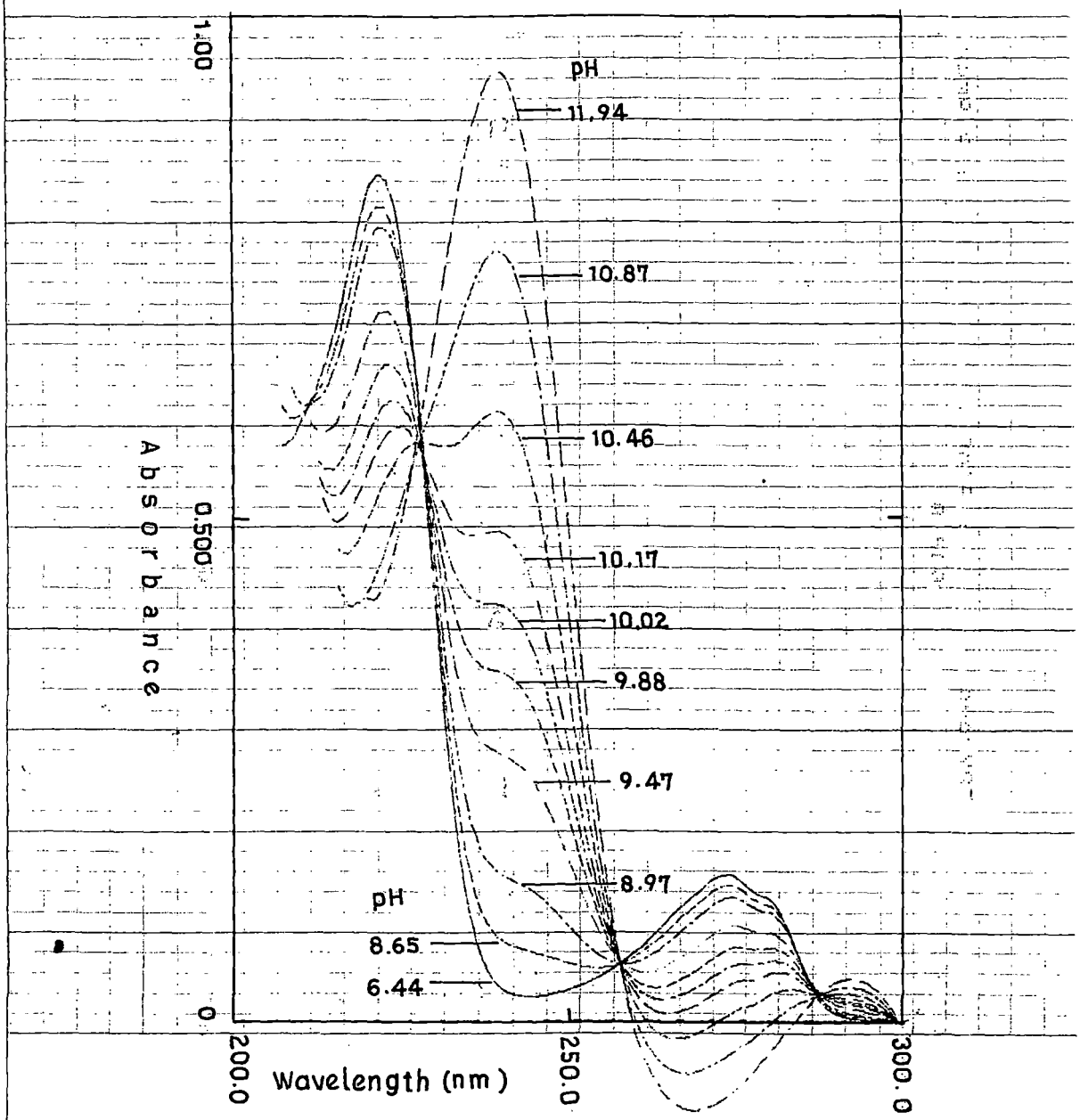

Fig.18. Absorption spectrum of L-Tyrosine methyl ester ($1x10^{-4}$M) in 0.01M Brij-35 solution.

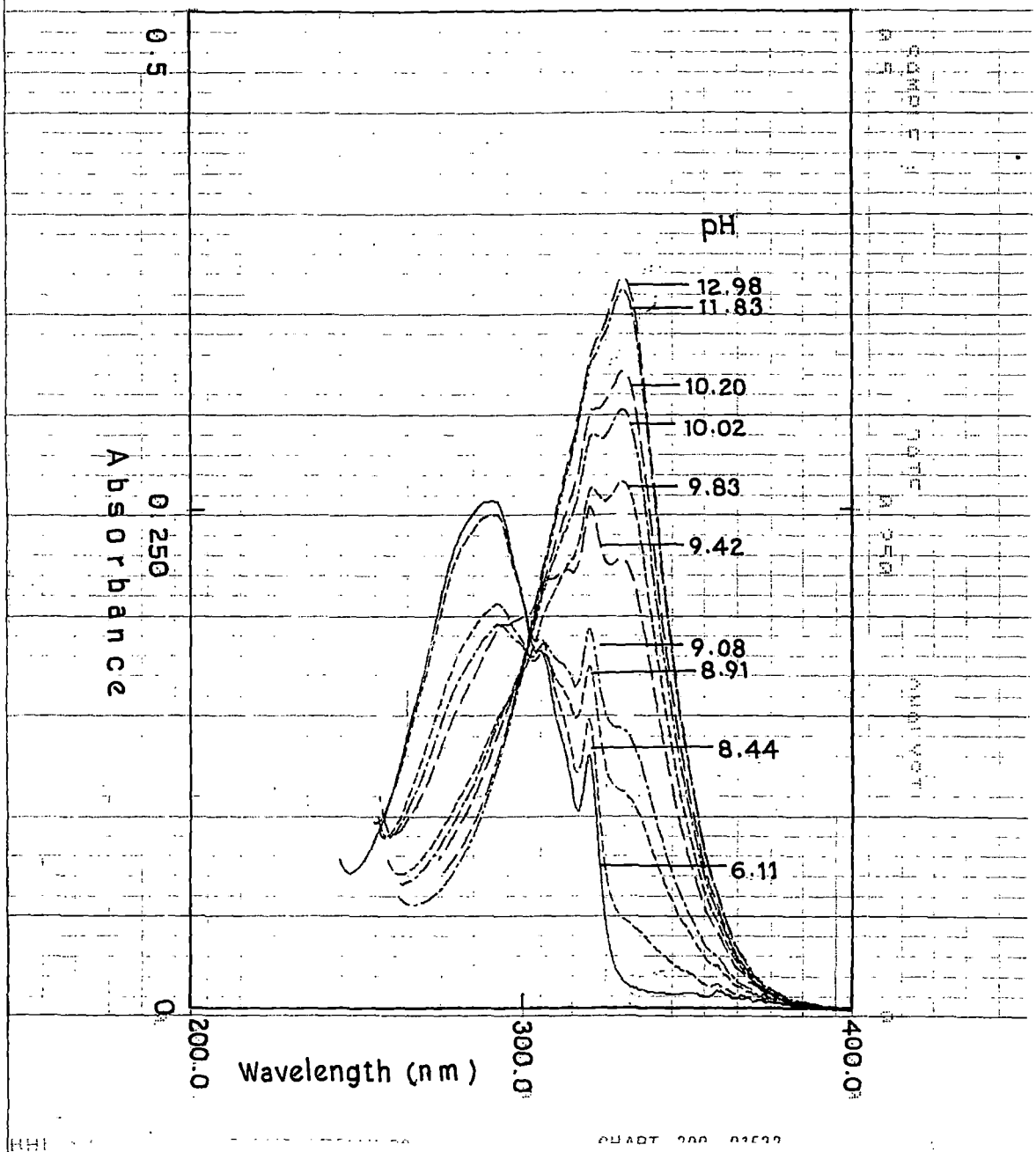

Fig.19. Absorption spectrum of 1-Naphthol ($0.5x10^{-4}$M) in water.

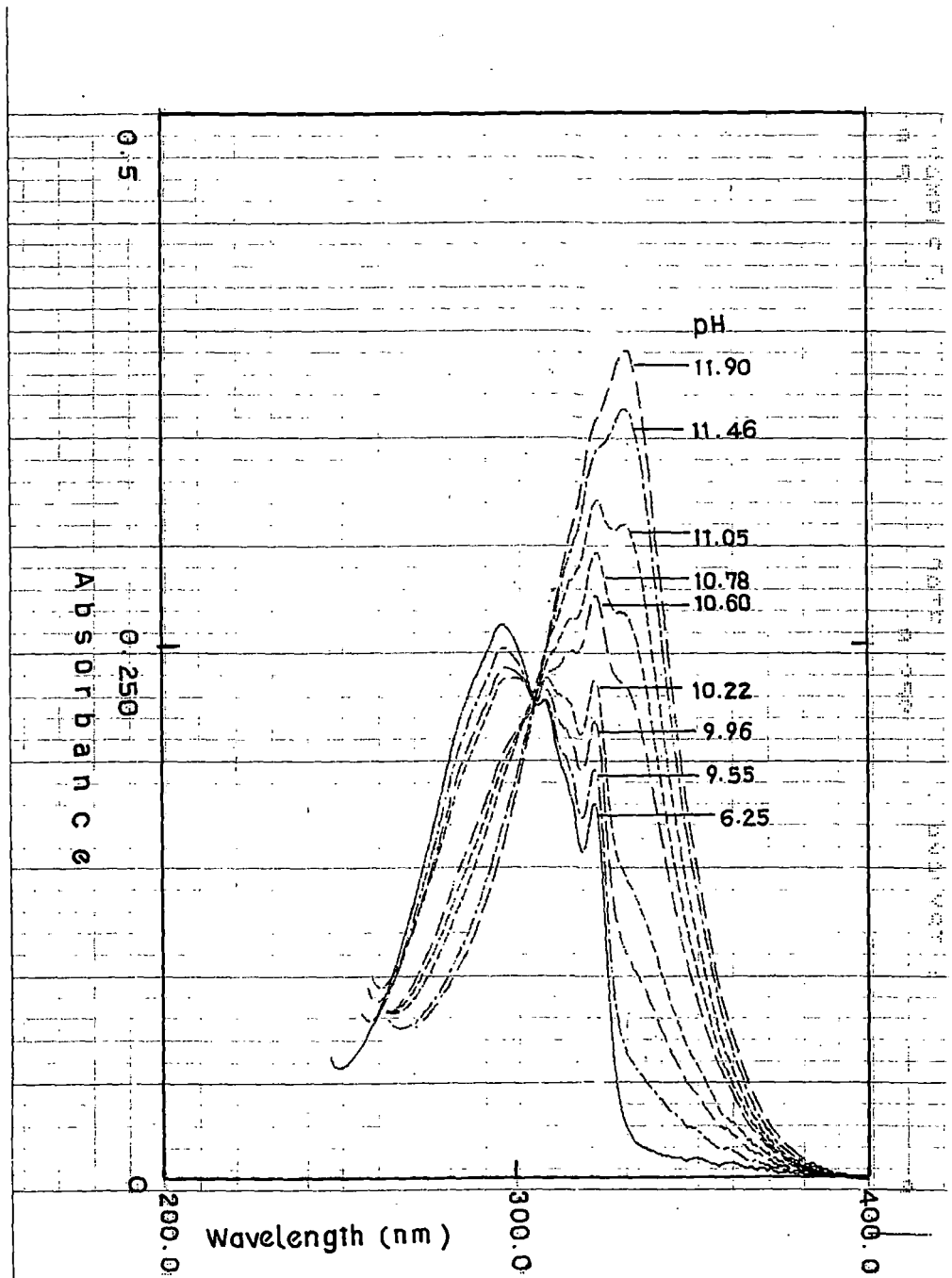

Fig.20. Absorption spectrum of 1-Naphthol ($0.5x10^{-4}$M) in 0.01M Brij-35 solution.

TABLE: 3

The position of the absorption band maximum of the conjugate acid-base forms of 5-Hydroxyindole

Medium	Dielectric Constant (D)	λ_{max} / nm	
		HIN	IN
Water	78.4	293	320
10% Dioxane	69.2	292	322
20% Dioxane	61.9	292	323
30% Dioxane	53.2	292	323
50% Dioxane	40.7	291	324
60% Dioxane	27.2	290	325
80% Dioxane	11.9	290	326
Tween-40	...	288	316
Brij-35	...	290	315
CTAB	...	290	324
SDS	...	290	316
AOT	...	292	315

TABLE: 4

The position of the absorption band maximum of the conjugate acid-base forms of 5-Hydroxy-L-tryptophan

Medium	Dielectric Constant (D)	λ_{max} / nm	
		HIN	IN
Water	78.4	296	322
10% Dioxane	69.2	295	322
20% Dioxane	61.9	295	323
30% Dioxane	53.2	294	323
50% Dioxane	40.7	294	324
60% Dioxane	27.2	294	325
80% Dioxane	11.9	294	326
Tween-40	...	295	322
Brij-35	...	295	322
CTAB	...	296	323
SDS	...	295	321
AOT	...	297	322

TABLE: 5

The position of the absorption band maximum of the conjugate acid-base forms of L-Tyrosine

Medium	Dielectric Constant (D)	λ_{max} / nm	
		HIN	IN
Water	78.4	242	270
10% Dioxane	69.2	240	272
20% Dioxane	61.9	239	273
30% Dioxane	53.2	237	275
50% Dioxane	40.7	236	276
60% Dioxane	27.2	236	277
80% Dioxane	11.9	238	278
Tween-40	...	238	276
Brij-35	...	235	275
CTAB	...	238	274
SDS	...	230	272
AOT	...	240	292

TABLE: 6

The position of the absorption band maximum of the conjugate acid-base forms of L-Tyrosinemethylester

Medium	Dielectric Constant (D)	λ_{max} / nm	
		HIN	IN
Water	78.4	240	274
10% Dioxane	69.2	237	275
20% Dioxane	61.9	236	276
30% Dioxane	53.2	235	276
50% Dioxane	40.7	234	277
60% Dioxane	27.2	233	277
80% Dioxane	11.9	231	278
Tween-40	...	238	276
Brij-35	...	235	275
CTAB	...	238	274
SDS	...	230	272
AOT	...	238	290

TABLE: 7

The position of the absorption band maximum of the conjugate acid-base forms of 1-Naphthol

Medium	Dielectric Constant (D)	λ_{max} / nm	
		HIN	IN
Water	78.4	298	334
10% Dioxane	69.2	295	331
20% Dioxane	61.9	294	335
30% Dioxane	53.2	293	336
50% Dioxane	40.7	292	337
60% Dioxane	27.2	292	339
80% Dioxane	11.9	290	341
Tween-40	...	295	322
Brij-35	...	296	332
CTAB	...	298	325
SDS	...	295	322
AOT	...	290	364

TABLE: 8

pH-Titration results for 5-Hydroxyindole in pure water and aqueous miceller solution with concentrations(M) at 298K

Medium	pK_a^{obs}	ΔpK_a^{obs}	pK_a^0	ΔpK_a^0
Water	11.041	–	–	–
0.001M CTAB	10.874	-0.167	13.258	2.217
0.01M CTAB	10.375	-0.666	12.759	1.718
0.02M CTAB	10.586	-0.455	12.970	1.929
0.05M CTAB	10.783	-0.258	13.167	2.126
0.1M CTAB	10.885	-0.156	13.269	2.228
0.001M SDS	10.802	-0.164	8.435	-2.606
0.01M SDS	11.328	0.287	8.961	-2.080
0.02M SDS	11.276	0.235	8.909	-2.132
0.05M SDS	11.464	0.423	9.097	-1.944
0.1M SDS	11.542	0.501	9.175	-1.866
0.001M Tween-40	11.026	-0.015	11.026	-0.015
0.01M Tween-40	11.135	0.094	11.135	0.094
0.02M Tween-40	11.154	0.113	11.154	0.113
0.05M Tween-40	11.598	0.557	11.598	0.557
0.1M Tween-40	11.677	0.636	11.677	0.636
0.001M Brij-35	11.180	0.139	11.180	0.139
0.01M Brij-35	11.299	0.258	11.299	0.258
0.02M Brij-35	11.532	0.491	11.532	0.491
0.03M Brij-35	11.537	0.496	11.537	0.496
0.001M AOT	10.767	-0.274	8.400	-2.641
0.01M AOT	10.589	-0.452	8.222	-2.819
0.02M AOT	10.586	-0.455	8.219	-2.822
0.03M AOT	10.534	-0.507	8.167	-2.874

TABLE: 9

pH-Titration results for 5-Hydroxy-L-tryptophan in pure water and aqueous miceller solution with concentrations(M) at 298K

Medium	pK_a^{obs}	ΔpK_a^{obs}	pK_a^0	ΔpK_a^0
Water	11.145	–	–	–
0.001M CTAB	10.771	-0.374	13.155	2.010
0.01M CTAB	10.344	-0.811	12.728	1.583
0.02M CTAB	10.598	-0.547	12.982	1.837
0.05M CTAB	10.516	-0.629	12.900	1.755
0.1M CTAB	10.814	-0.331	13.198	2.053
0.001M SDS	10.783	-0.362	8.416	-2.729
0.01M SDS	11.267	0.122	8.900	-2.245
0.02M SDS	11.321	0.176	8.954	-2.191
0.05M SDS	11.353	0.208	8.986	-2.159
0.1M SDS	11.290	0.145	8.923	-2.222
0.001M Tween-40	11.072	-0.073	11.072	-0.073
0.01M Tween-40	11.093	-0.052	11.093	-0.052
0.02M Tween-40	11.134	-0.011	11.134	-.011
0.05M Tween-40	10.912	-0.233	10.912	-0.233
0.1M Tween-40	11.326	-0.181	11.326	0.181
0.001M Brij-35	11.331	0.186	11.331	0.186
0.01M Brij-35	11.240	0.095	11.240	0.095
0.02M Brij-35	11.280	0.135	11.280	0.135
0.03M Brij-35	11.323	0.178	11.323	0.178
0.001M AOT	10.750	-0.395	8.383	-2.762
0.01M AOT	10.600	-0.546	8.233	-2.912
0.02M AOT	10.684	-0.462	8.317	-2.828
0.03M AOT	10.666	-0.479	8.299	-2.846

TABLE: 10

pH-Titration results for L-Tyrosine in pure water and aqueous miceller solution with concentrations(M) at 298K

Medium	pK_a^{obs}	ΔpK_a^{obs}	pK_a^0	ΔpK_a^0
Water	10.052	–	–	–
0.001M CTAB	9.755	-0.297	12.139	2.087
0.01M CTAB	9.514	-0.538	11.898	1.846
0.02M CTAB	9.599	-0.453	11.983	1.931
0.05M CTAB	9.630	-0.422	12.041	1.989
0.1M CTAB	9.756	-0.296	12.140	2.088
0.001M SDS	9.988	-0.064	7.621	-2.437
0.01M SDS	10.023	-0.029	7.656	-2.402
0.02M SDS	9.784	-0.268	7.417	-2.641
0.05M SDS	10.156	0.104	7.789	-2.269
0.1M SDS	9.968	-0.084	7.601	-2.457
0.001M Tween-40	10.241	0.189	10.241	0.189
0.01M Tween-40	10.217	0.165	10.217	0.165
0.02M Tween-40	10.207	0.155	10.207	0.155
0.001M Brij-35	10.081	0.029	10.081	0.029
0.01M Brij-35	10.089	0.037	10.089	0.037
0.02M Brij-35	10.112	0.600	10.112	0.060
0.03M Brij-35	10.451	0.399	10.451	0.399
0.001M AOT	10.226	0.174	7.859	-2.153
0.01M AOT	10.084	0.316	7.717	-2.335
0.02M AOT	10.154	0.102	7.787	-2.265
0.03M AOT	9.726	-0.326	7.359	-2.693

TABLE: 11

pH-Titration results for L-Tyrosinemethylester in pure water and aqueous miceller solution with concentrations(M) at 298K

Medium	pK_a^{obs}	ΔpK_a^{obs}	pK_a^0	ΔpK_a^0
Water	10.087	–	–	–
0.001M CTAB	9.883	-0.204	12.267	2.180
0.01M CTAB	9.503	-0.583	11.887	1.800
0.02M CTAB	9.610	-0.477	11.994	1.907
0.05M CTAB	9.711	-0.376	12.095	2.008
0.1M CTAB	9.411	-0.676	11.795	1.708
0.001M SDS	9.938	-0.149	7.571	-2.516
0.01M SDS	10.095	0.008	7.728	-2.359
0.02M SDS	10.028	-0.059	7.661	-2.426
0.05M SDS	10.123	0.036	7.756	-2.331
0.1M SDS	9.981	-0.106	7.614	-2.473
0.001M Tween-40	10.008	-0.079	10.008	-0.079
0.01M Tween-40	10.232	-0.145	10.232	0.145
0.02M Tween-40	10.052	-0.035	10.052	-0.035
0.001M Brij-35	10.132	0.045	10.132	0.045
0.01M Brij-35	10.177	0.090.	10.177	0.090
0.02M Brij-35	10.270	0.183	10.270	0.183
0.03M Brij-35	10.393	0.306	10.393	0.306
0.001M AOT	9.978	-0.109	7.611	-2.476
0.01M AOT	9.940	-0.147	7.573	-2.514
0.02M AOT	9.789	-0.298	7.422	-2.665
0.03M AOT	9.789	-0.298	7.422	-2.665

TABLE: 12

pH-Titration results for 1-Naphthol in pure water and aqueous miceller solution with concentrations(M) at 298K

Medium	pK_a^{obs}	ΔpK_a^{obs}	pK_a^0	ΔpK_a^0
Water	9.388	–	–	–
0.001M CTAB	8.387	-1.001	10.771	1.383
0.01M CTAB	8.023	-1.365	10.407	1.019
0.02M CTAB	8.623	-1.765	11.007	1.619
0.05M CTAB	8.679	0.709	11.063	1.675
0.1M CTAB	8.914	0.474	11.298	1.910
0.001M SDS	9.666	0.278	7.299	-2.089
0.01M SDS	9.459	0.071	7.092	-2.296
0.02M SDS	10.132	0.744	7.765	-1.623
0.05M SDS	10.415	1.027	8.048	-1.340
0.1M SDS	9.925	0.537	7.558	-1.830
0.001M Tween-40	9.644	0.256	9.644	0.256
0.01M Tween-40	9.601	0.308	9.601	0.213
0.02M Tween-40	10.868	1.480	10.868	1.480
0.05M Tween-40	10.798	1.401	10.798	1.410
0.001M Brij-35	9.971	0.583	9.971	0.583
0.01M Brij-35	10.563	1.175	10.563	1.175
0.02M Brij-35	10.829	1.441	10.829	1.441
0.03M Brij-35	11.025	1.637	11.025	1.637
0.001M AOT	9.369	-0.019	7.002	-2.386
0.01M AOT	9.499	0.111	7.132	-2.256
0.02M AOT	9.805	0.417	7.438	-1.950
0.03M AOT	9.447	0.059	7.080	-2.308

TABLE: 13

5-Hydroxyindole in 1,4-Dioxane-water Mixtures

Dioxane %	D_{eff}	pK_a^m	ΔpK_a^m	pK_a^i	ΔpK_a^i
10%	69.2	11.395	0.354	12.395	1.354
20%	61.9	11.767	0.726	12.587	1.546
30%	53.2	12.302	1.261	12.902	1.861
50%	40.7	13.233	2.192	13.423	2.382
60%	27.2	13.972	2.931	13.992	2.951
80%	11.9	16.213	5.172	15.833	4.792

TABLE: 14

5-Hydroxy-L-tryptophan in 1,4-Dioxane-water Mixtures

Dioxane %	D_{eff}	pK_a^m	ΔpK_a^m	pK_a^i	ΔpK_a^i
10%	69.2	11.608	0.463	12.395	1.463
20%	61.9	12.017	0.872	12.837	1.692
30%	53.2	12.442	1.297	13.042	1.897
50%	40.7	13.435	2.290	13.625	2.480
60%	27.2	13.968	2.823	13.988	2.843
80%	11.9	15.630	4.485	15.250	4.105

TABLE: 15

L-Tyrosine in 1,4-Dioxane-water Mixtures

Dioxane %	D_{eff}	pK_a^m	ΔpK_a^m	pK_a^i	ΔpK_a^i
10%	69.2	10.503	0.451	11.503	1.451
20%	61.9	10.898	0.846	11.718	1.666
30%	53.2	11.274	1.222	11.847	1.822
50%	40.7	12.519	2.467	12.709	2.657
60%	27.2	13.234	3.182	13.254	3.202
80%	11.9	15.066	5.014	14.686	4.634

TABLE: 16

L-Tyrosinemethylester in 1,4-Dioxane-water Mixtures

Dioxane %	D_{eff}	pK_a^m	ΔpK_a^m	pK_a^i	ΔpK_a^i
10%	69.2	10.600	0.513	11.600	1.513
20%	61.9	10.686	0.599	11.506	1.419
30%	53.2	11.350	1.263	11.950	1.863
50%	40.7	12.413	2.326	12.603	2.516
60%	27.2	13.093	3.006	13.113	3.026
80%	11.9	15.599	5.512	15.219	5.132

TABLE: 17

1-Naphthol in 1,4-Dioxane-water Mixtures

Dioxane %	D_{eff}	pK_a^m	ΔpK_a^m	pK_a^i	ΔpK_a^i
10%	69.2	9.712	0.324	10.712	1.324
20%	61.9	10.126	0.738	10.946	1.558
30%	53.2	10.574	1.186	11.174	1.786
50%	40.7	11.459	2.071	11.649	2.261
60%	27.2	11.783	2.395	11.803	2.415
80%	11.9	13.978	4.590	13.598	4.210

TABLE: 18

Values of effective dielectric constant (D_{eff}) for 5-Hydroxyindole in CTAB

Medium	D_{eff}
0.001M CTAB	38.8
0.01M CTAB	52.2
0.02M CTAB	46.3
0.05M CTAB	40.5
0.1M CTAB	37.8

TABLE: 19

Values of effective dielectric constant (D_{eff}) for 5-Hydroxy-L-tryptophan in CTAB

Medium	D_{eff}
0.001M CTAB	47.5
0.01M CTAB	68.1
0.02M CTAB	53.4
0.05M CTAB	59.8
0.1M CTAB	47.1

TABLE: 20

Values of effective dielectric constant (D_{eff}) for L-Tyrosine in CTAB

Medium	D_{eff}
0.001M CTAB	44.6
0.01M CTAB	53.1
0.02M CTAB	52.1
0.05M CTAB	51.7
0.1M CTAB	44.5

TABLE: 21

Values of effective dielectric constant (D_{eff}) for L-Tyrosinemethylester in CTAB

Medium	D_{eff}
0.001M CTAB	43.5
0.01M CTAB	52.5
0.02M CTAB	51.5
0.05M CTAB	44.7
0.1M CTAB	56.9

TABLE: 22

Values of effective dielectric constant (D_{eff}) for 1-Naphthol in CTAB

Medium	D_{eff}
0.001M CTAB	60.0
0.01M CTAB	50.0
0.02M CTAB	50.0
0.05M CTAB	45.0
0.1M CTAB	45.0

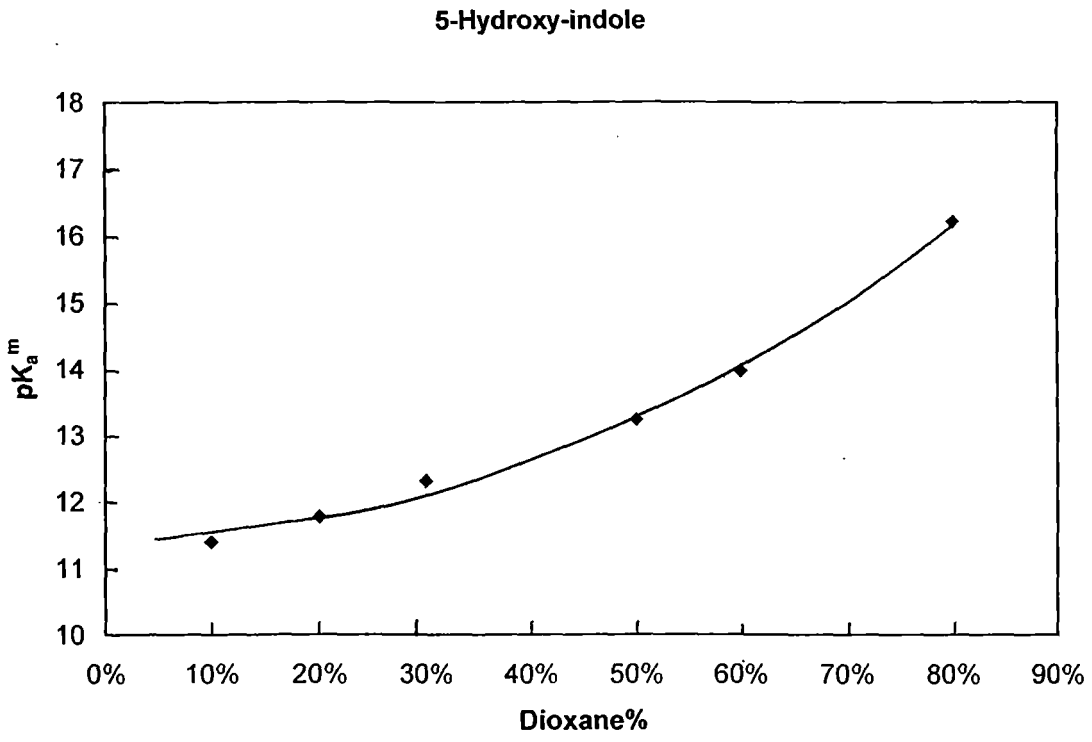

Fig.21.Plot of pK_a^m versus dioxane% of dioxane-water mixtures

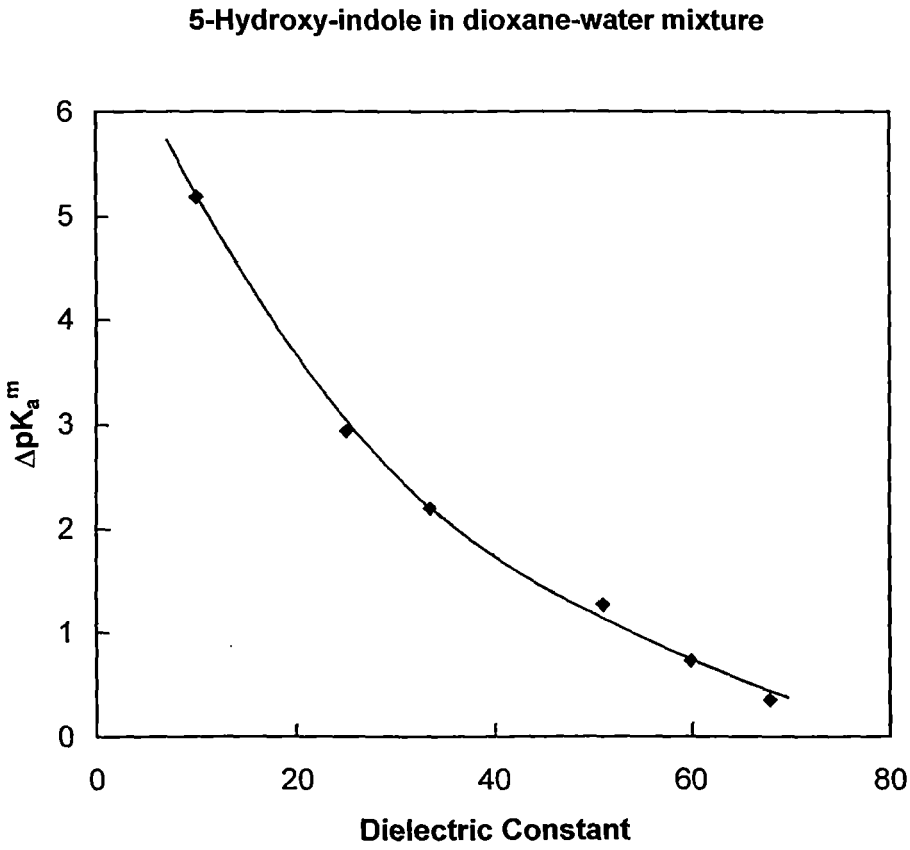

Fig.22.Plot of ΔpK_a^m versus dielectric constant of dioxane-water mixtures.

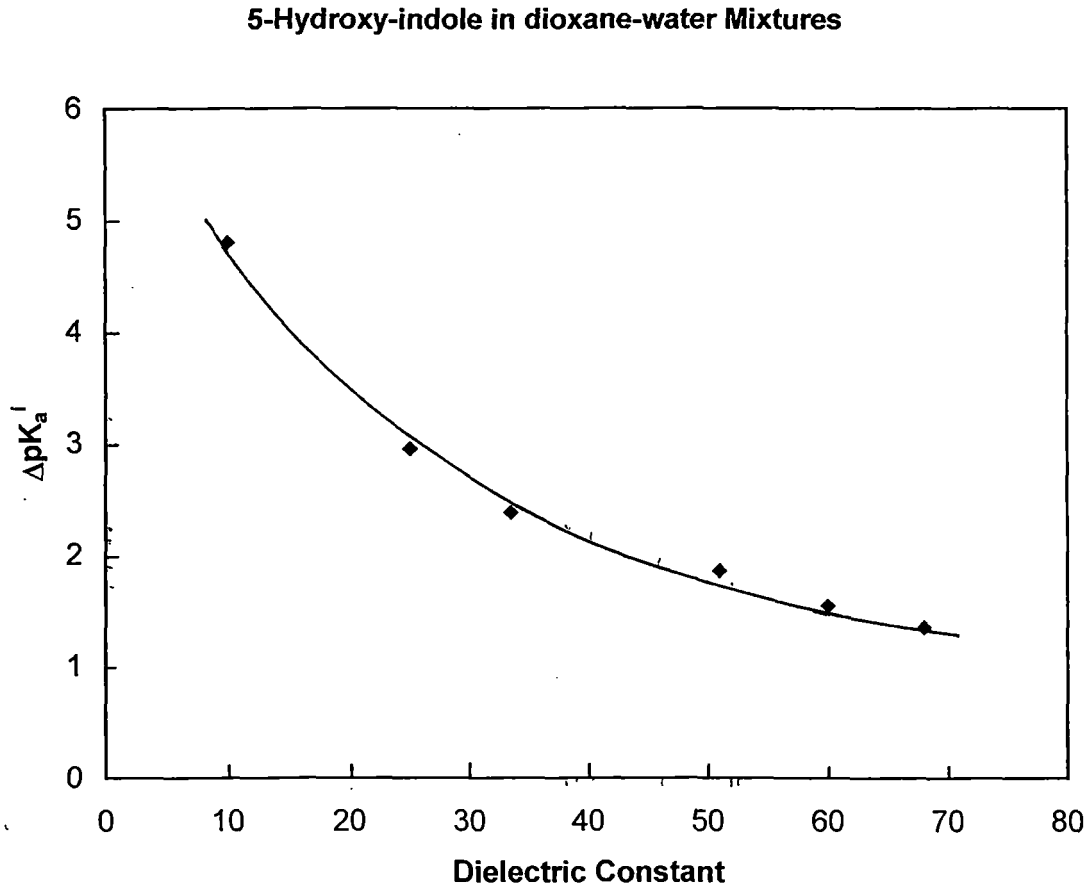

Fig.23.Plot of ΔpK_a^i versus dielectric constant of dioxane-water mixtures.

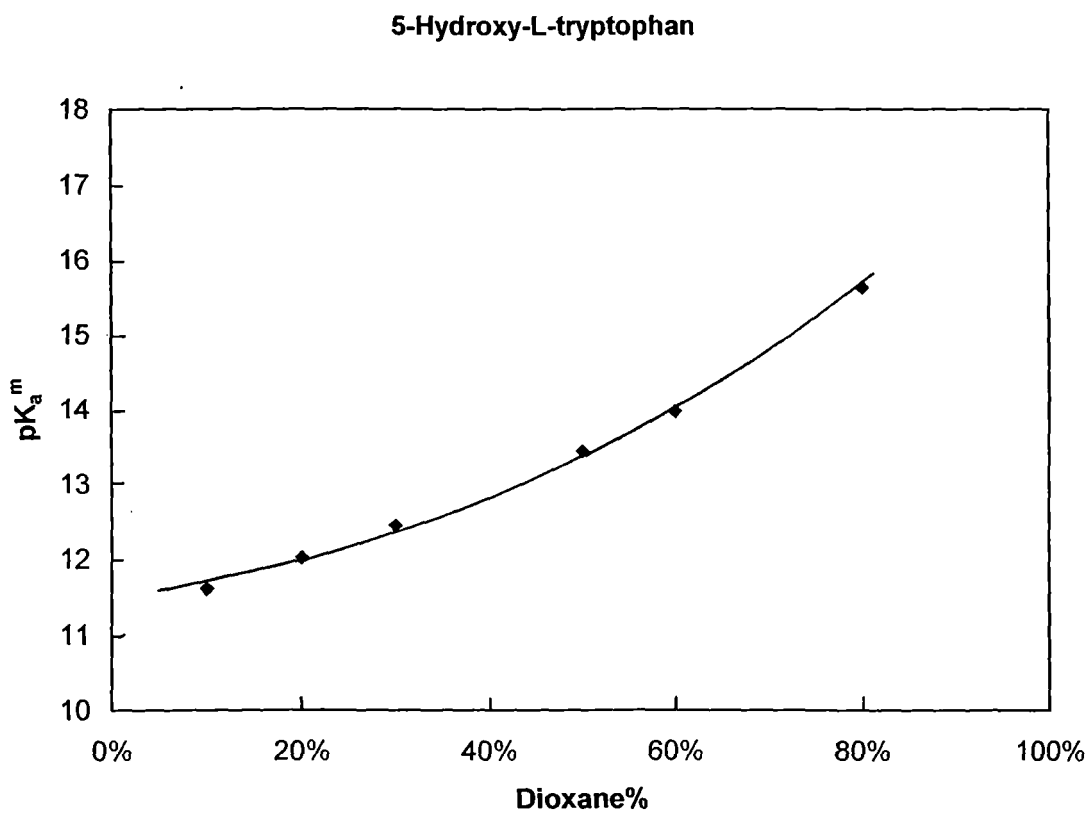

Fig.24.Plot of pK_a^m versus dioxane% of dioxane-water mixtures

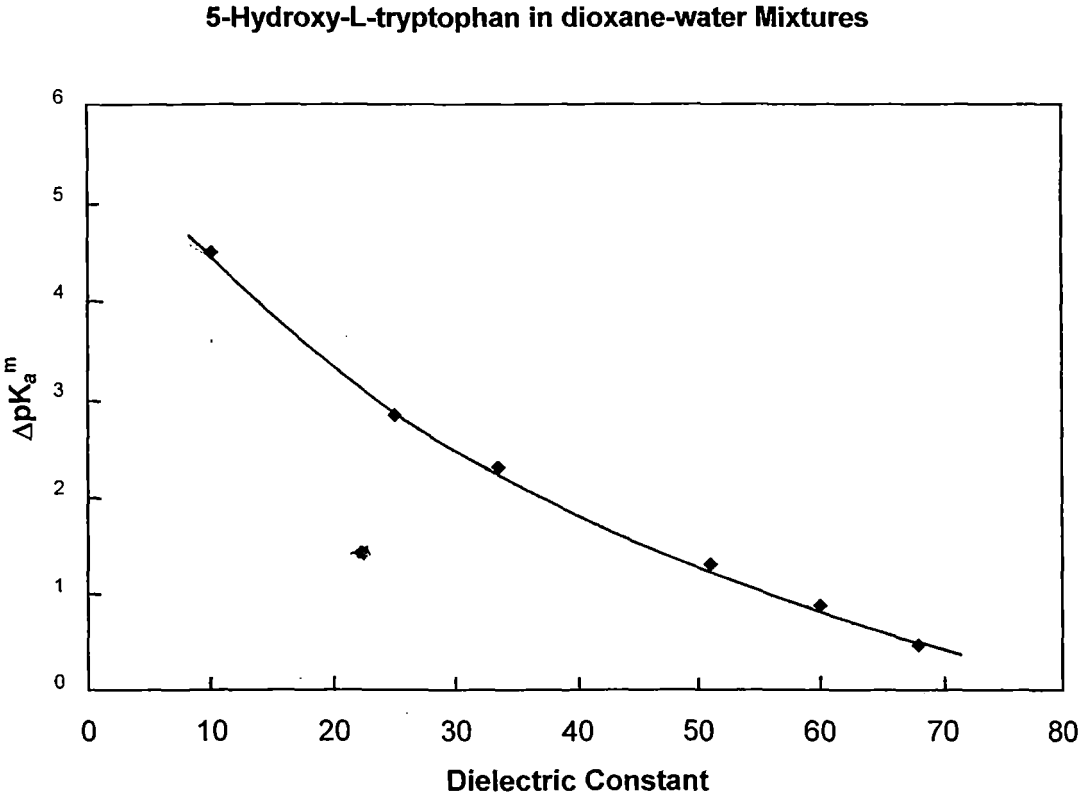

Fig.25.Plot of ΔpK_a^m versus dielectric constant of dioxane-water mixtures.

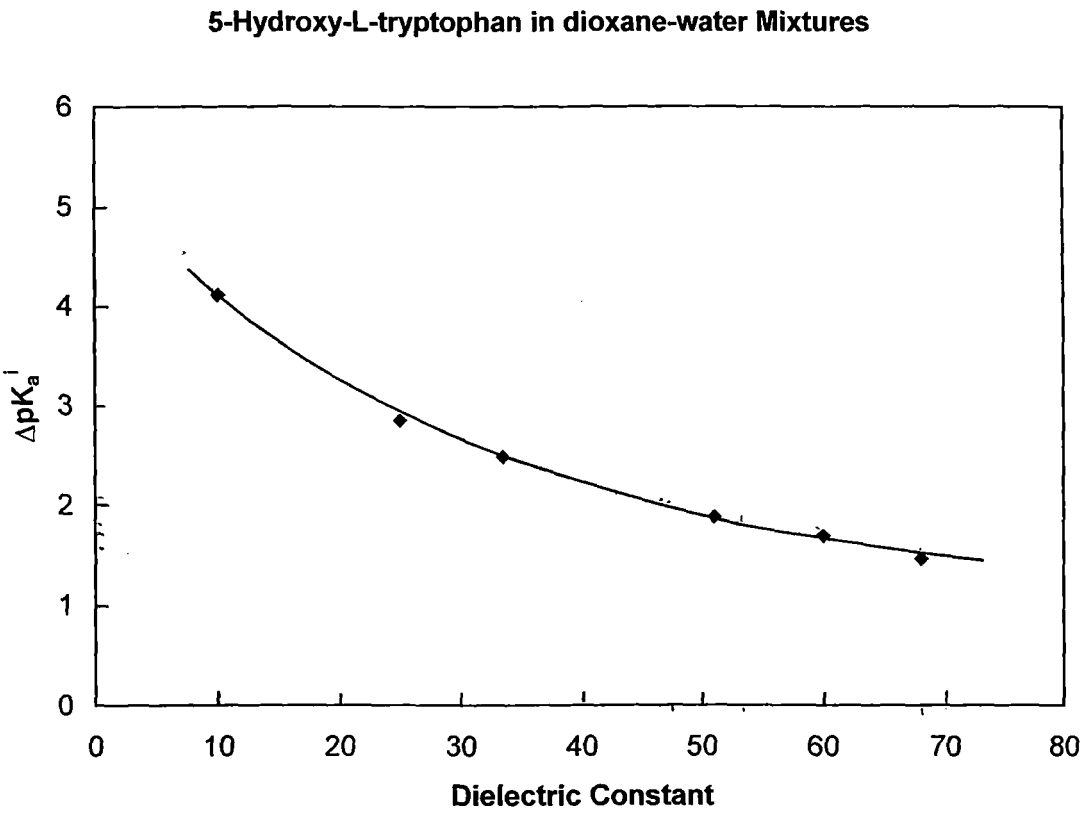

Fig.26.Plot of ΔpK_a^i versus dielectric constant of dioxane-water mixtures.

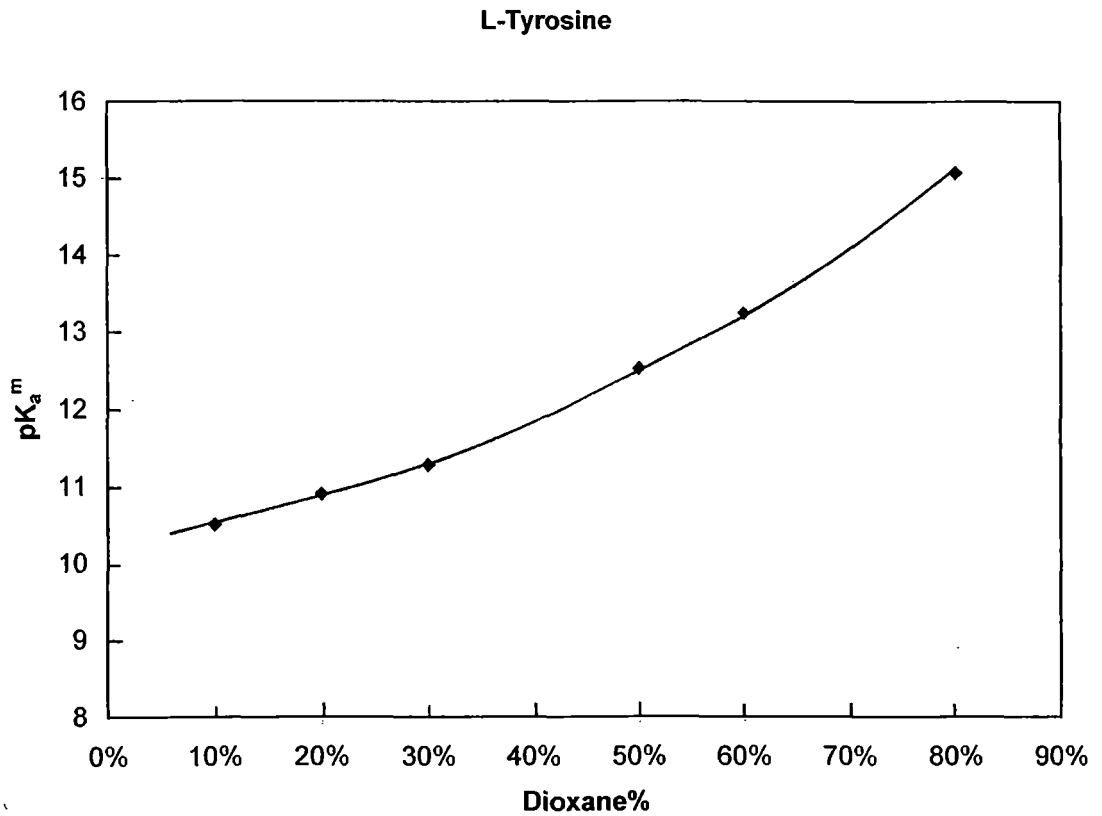

Fig.27 Plot of pK_a^m versus dioxane% of dioxane-water mixtures

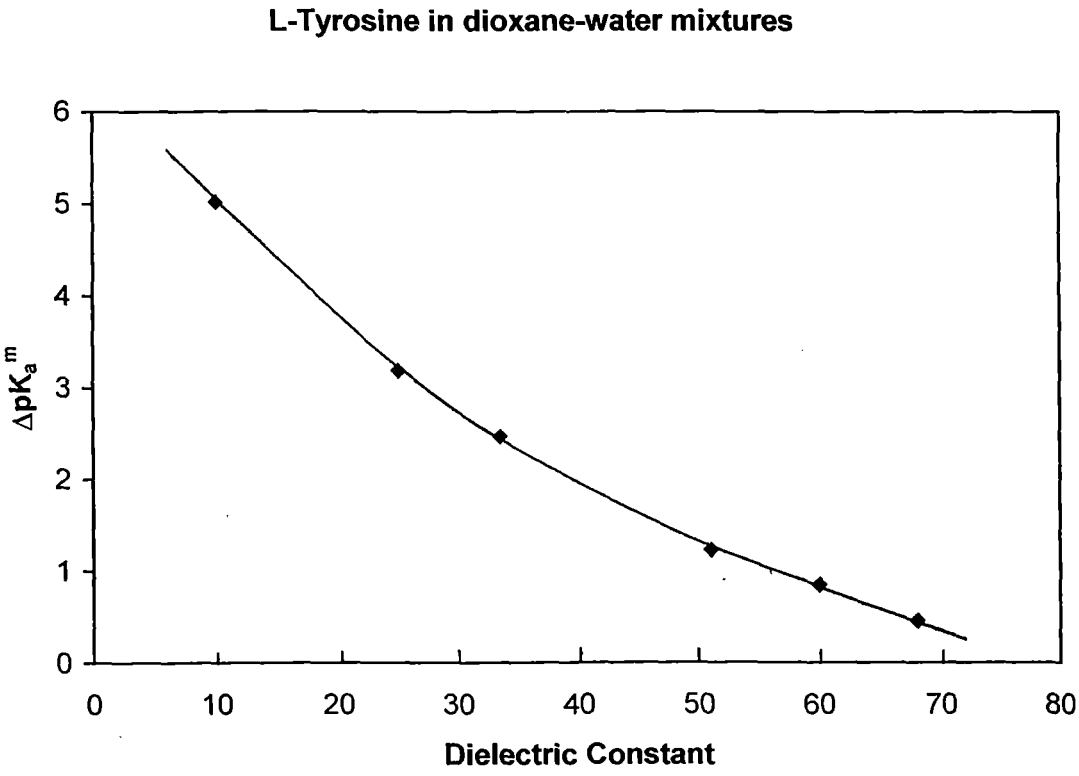

Fig.28.Plot of ΔpK_a^m versus dielectric constant of dioxane-water mixtures.

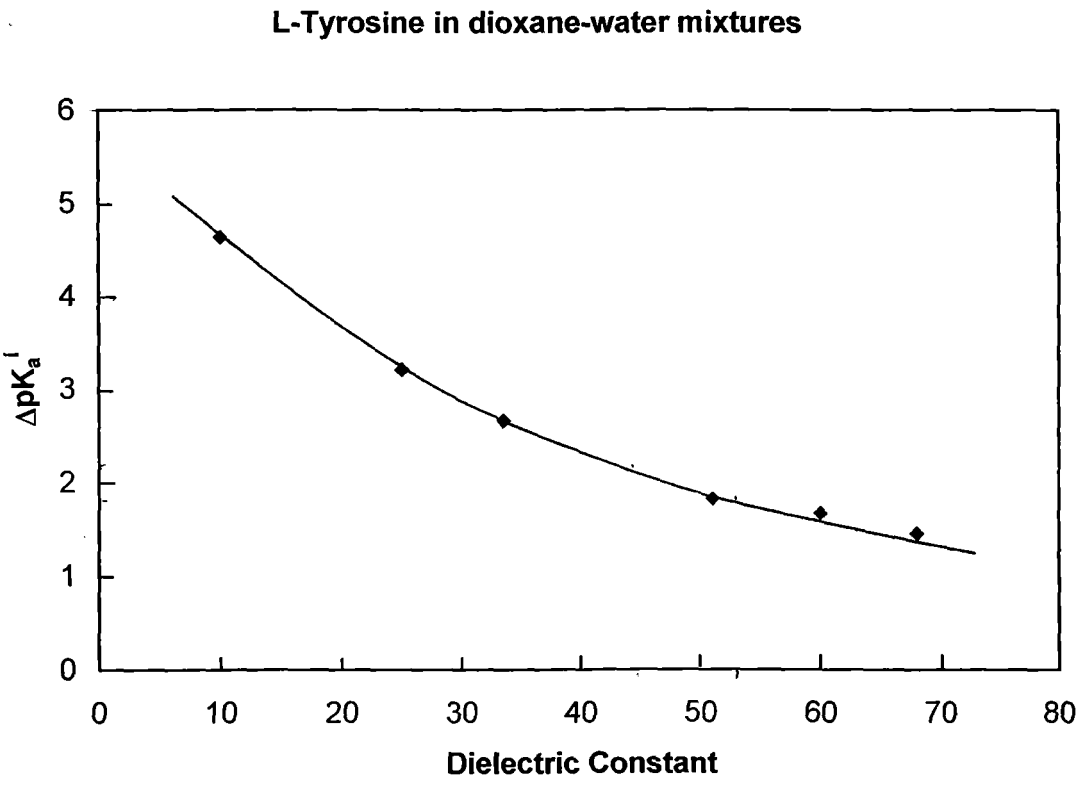

Fig. 29. Plot of ΔpK_a^i versus dielectric constant of dioxane-water mixtures.

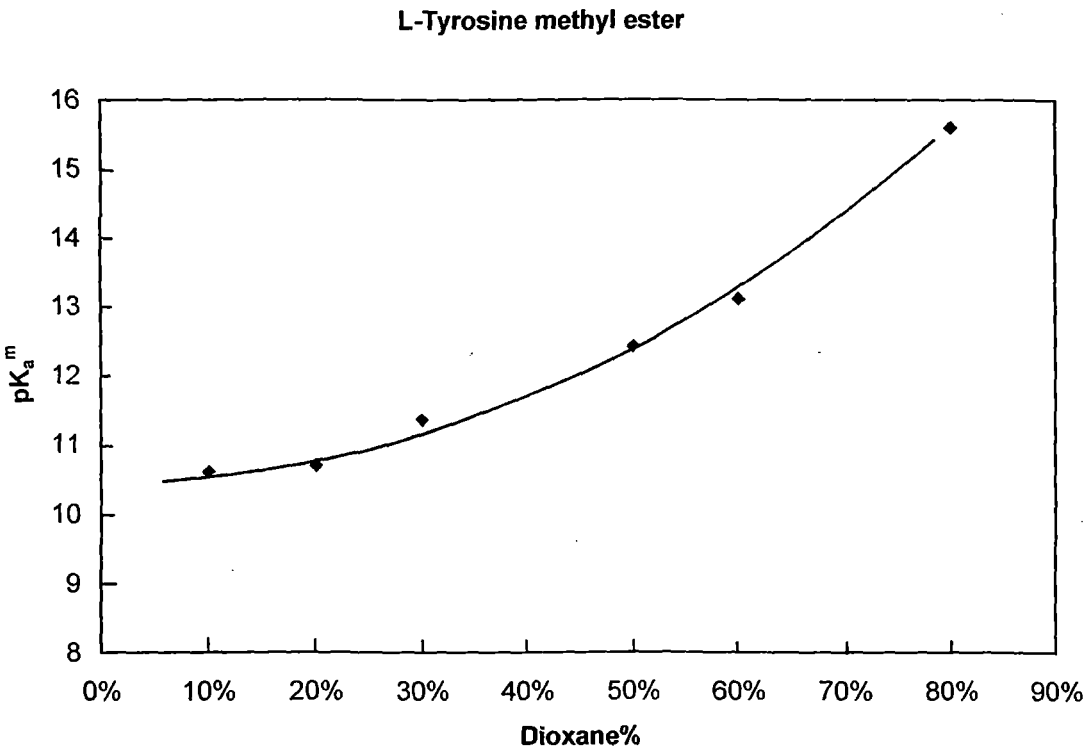

Fig.30.Plot of pK_a^m versus dioxane% of dioxane-water mixtures

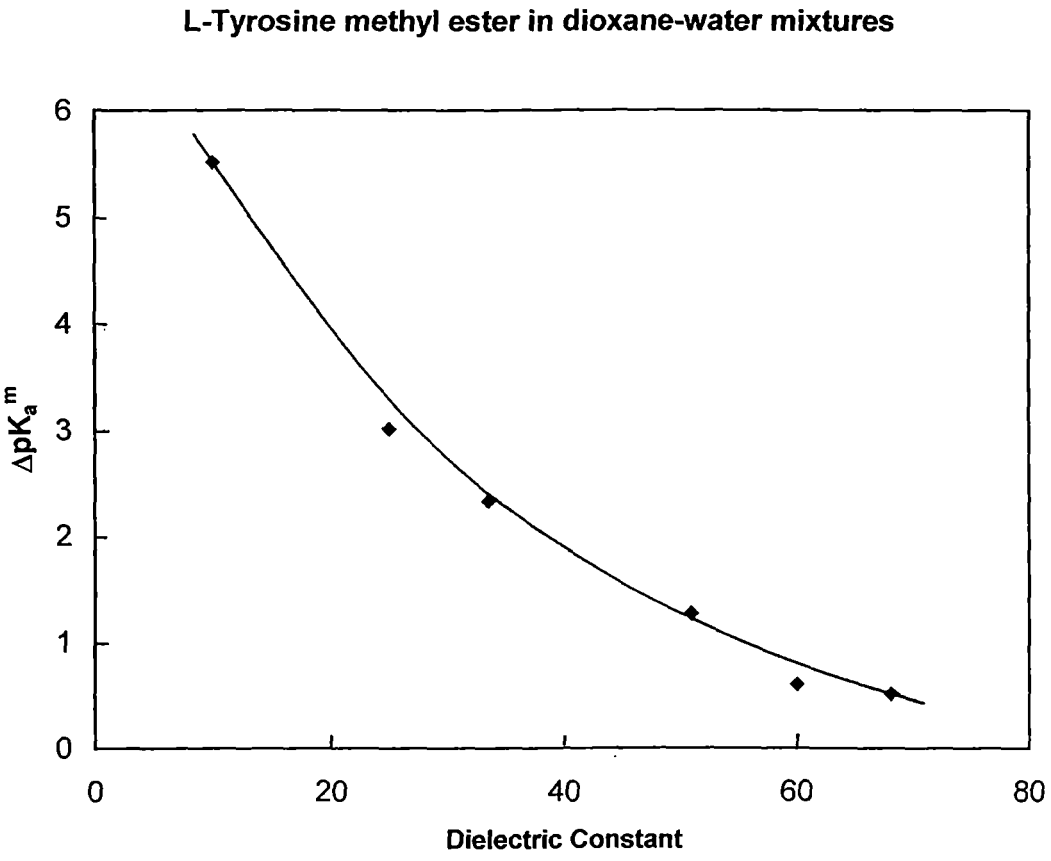

Fig.31.Plot of ΔpK_a^m versus dielectric constant of dioxane-water mixtures.

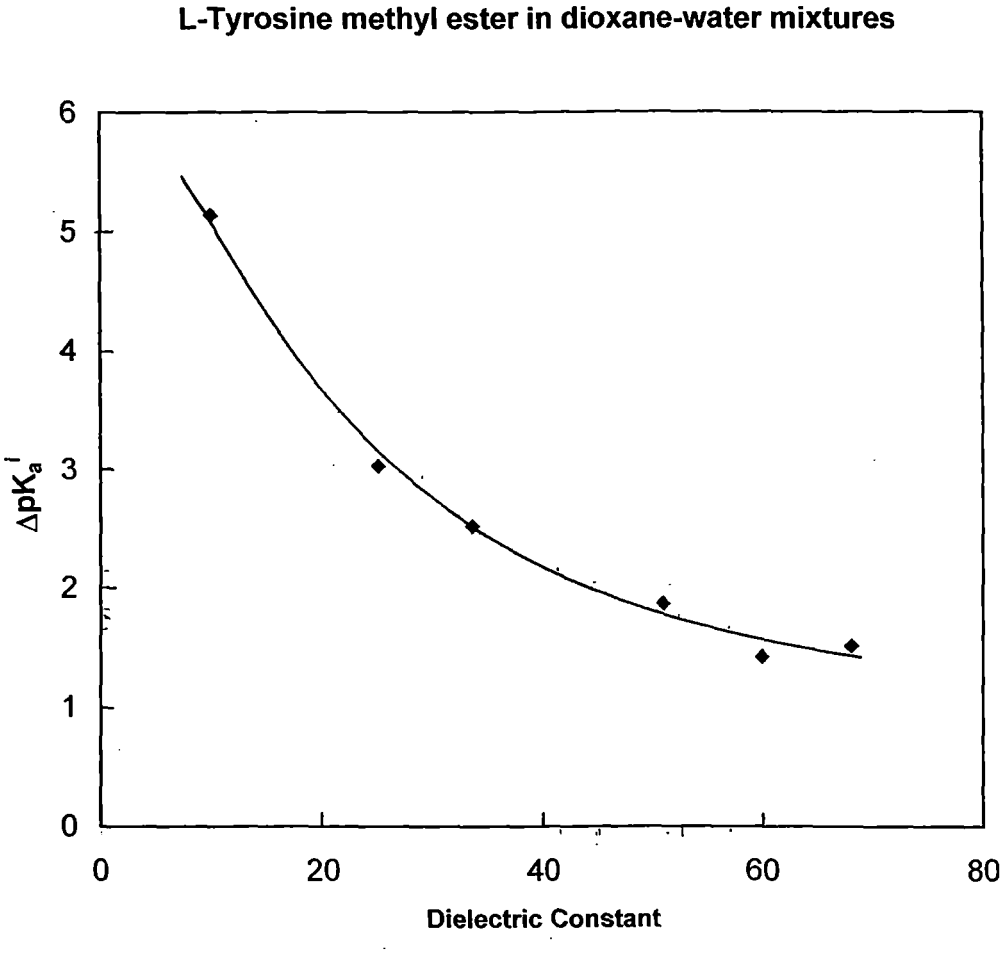

Fig.32.Plot of ΔpK_a^i versus dielectric constant of dioxane-water mixtures.

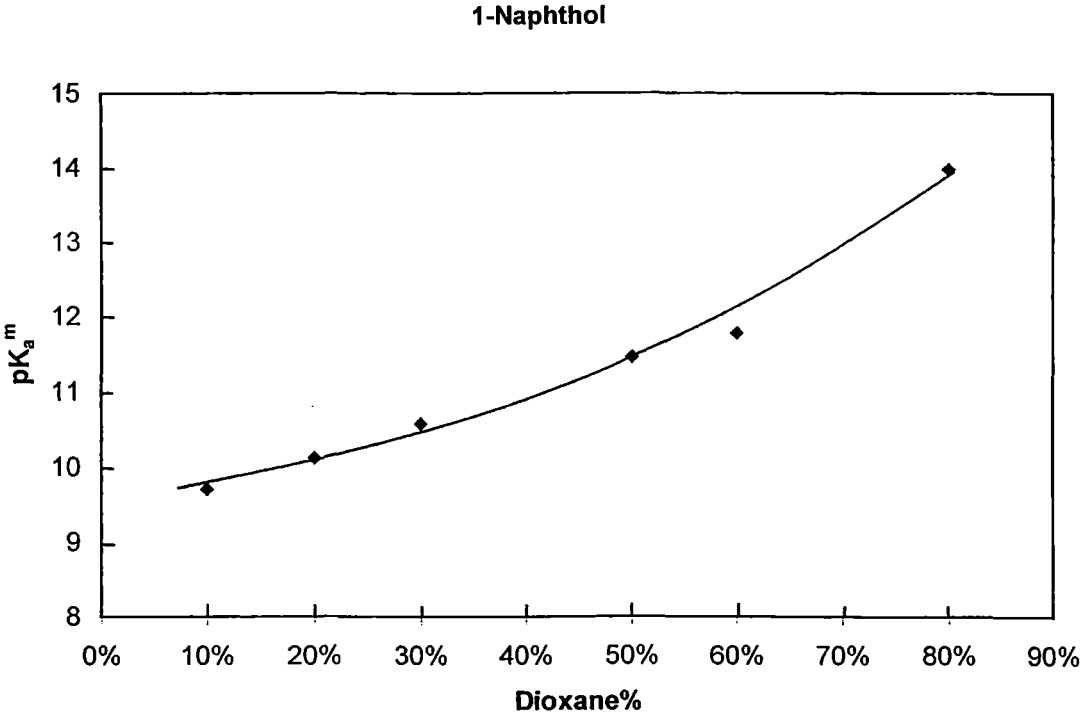

Fig.33.Plot of pK_a^m versus dioxane% of dioxane-water mixtures.

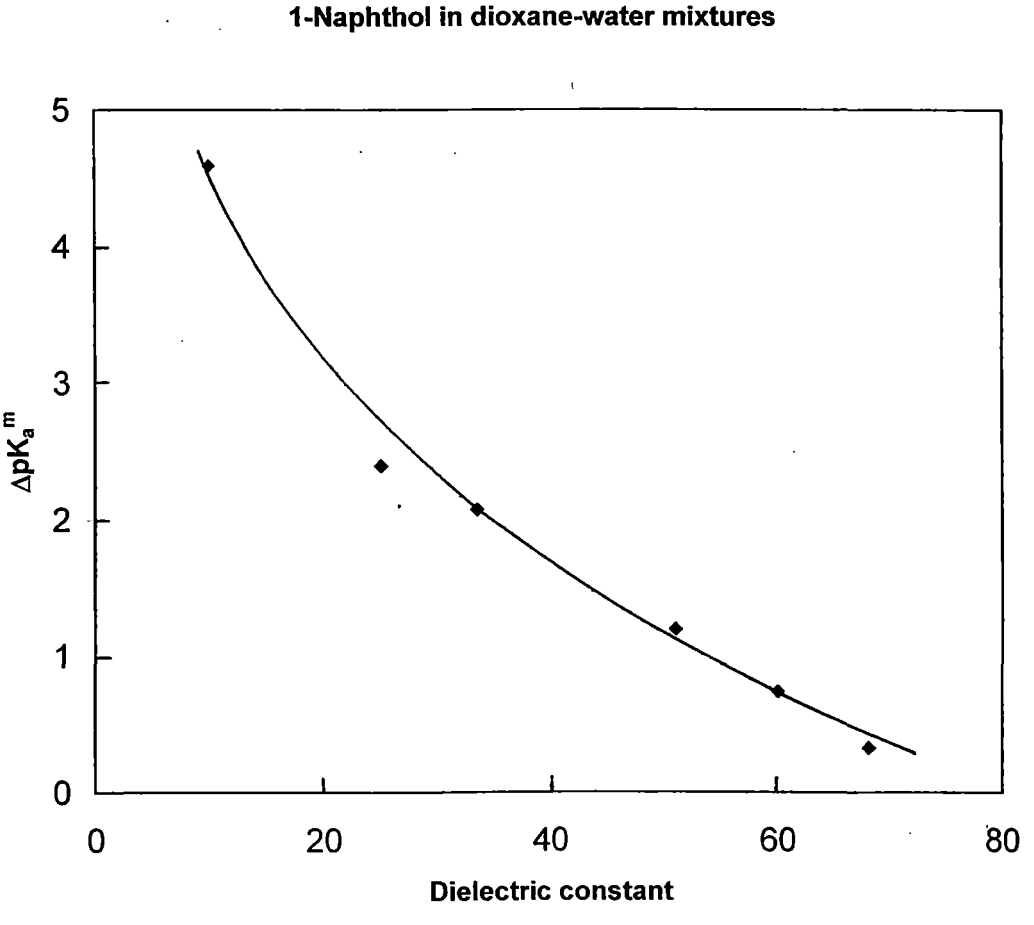

Fig.34.Plot of ΔpK_a^m versus dielectric constant of dioxane-water mixtures.

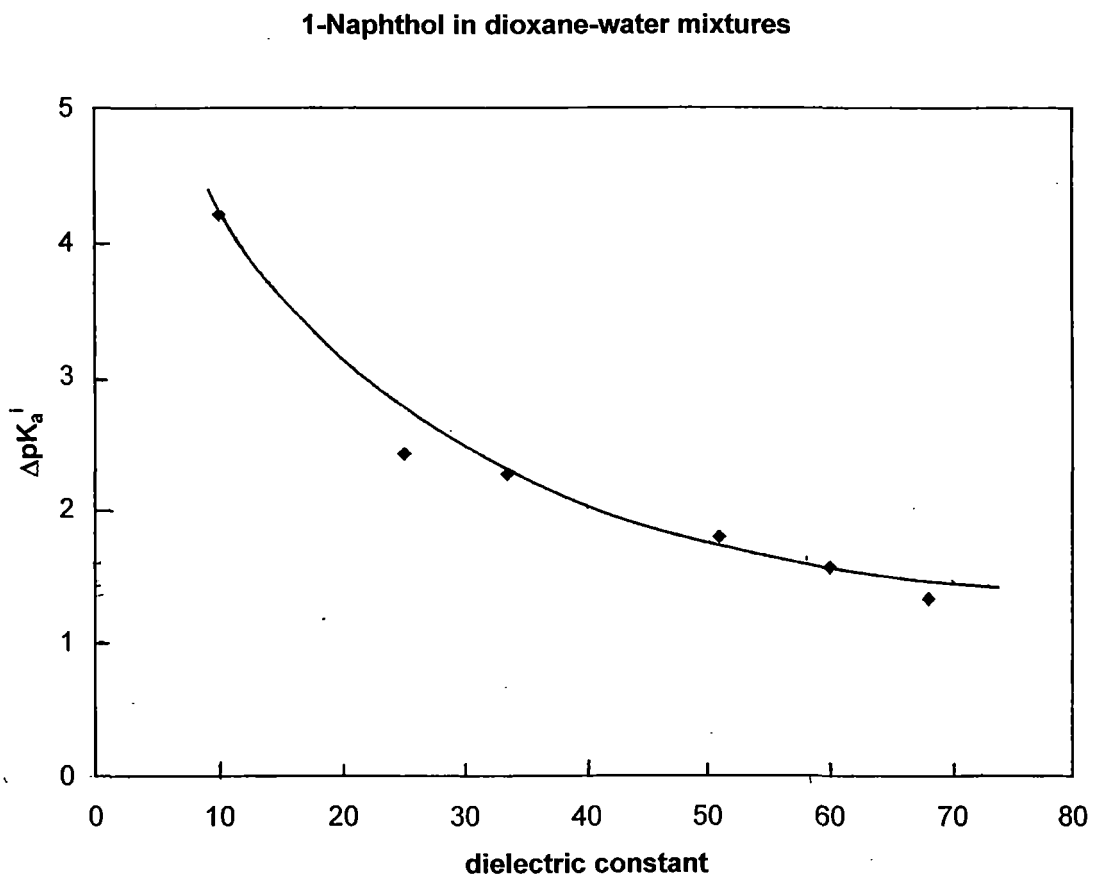

Fig.35.Plot of ΔpK_a^i versus dielectric constant of dioxane-water mixtures.

References

1. Hartley, G. S., *Quart. Rev.*, **2**, 152 (1948).
2. Hartley, G. S., *Micellization, Solubilisation and Microemulsions*, Ed. Mittal, K. L., Plenum New York, 23 (1977).
3. Fendler, J. H., Fendler, E. J., *Catalysis in Micellar and Macromolecular Systems*, Academic Press, New York, 48 (1975).
4. Fendler, J. H., *Membrane Mimetic Chemistry*, Wiley Interscience, New York (1982).
5. Lindman, B., Wennerström, H., *Top. Curr. Chem.*, **87**, 1 (1980).
6. Sudhölter, E. J. R., van der Langkruis, G. B., EngBerts, J. B. F. N., *Recl. Trav. Chim. Pay-Bas Belg*, **99**, 73 (1979).
7. Brown, J. M., Colloid Science, A. *Specialist Periodical Report*, Chemical Society, London, **3**, 253 (1979).
8. Kunitake, T., Shinkai, S., *Adv. Phys. Org. Chem.*, **17**, 435 (1980).
9. Ray, A., *Nature*, **231**, 313 (1971).
10. Ray, A., Nemethy, G., *J. Phys. Chem.*, **75**, 809 (1971).
11. Ionescu, L. G., Fung, D. S., *J. Chem., Soc., Faraday Trans. I*, **77**, 2907 (1981).
12. Evans, D. F., Nimham, B. W., *J. Phys. Chem.*, **87**, 5025 (1983).
13. Menger, F. M., Jerkunica, J. M., J. *Am. Chem. Soc.*, **101**, 1896 (1979).
14. Tanford, C., *The Hydrophobic Effect*, 2nd Edn., Wiley Interscience, New York, (1980).
15. Debye. P., *J. Phys. Colloid Chem.*, **53**, 1 (1949).
16. Debye. P., Anacker, E. W., *J. Phys. Colloid Chem.*, **55**, 644 (1951).
17. Mukherjee, P., Mysels, K. J., *Critical Micelle Concentrations of Aqueous Surfactant Systems*, National Bureau of Standerds, Washington D. C., (1970).
18. Menger, F. M., Portnoy, C. E., *J. Am. Chem. Soc.*, **89**, 4698 (1967).

19. Gunnarsson, G., Jonsson, B., Wennerström, H., *J. Phys. Chem.*, **84**, 3114 (1980).
20. Duynstee, E. F. J., Grunwald, E., *J. Am. Chem. Soc.*, **81**, 4540, 4542 (1959).
21. Kurz, J. L., *J. Phys. Chem.*, **66**, 2239 (1962).
22. Motsavage, V. A., Kostenbauder, H. B., *J. Colloid Sci.*, **18**, 603 (1963).
23. Bellocq, A. M., Biais, J., Bothorel, P., Clin, B., Fourche, G., Lalanne, P., Lemaire, B., Lemanceau, B., Roux, D., *Adv. Colloid Interface Sci.*, **20**, 167 (1984).
24. Mackay, R. A., *Adv. Colloid Interface Sci.*, **15**, 131 (1981).
25. Zana, R., Yiv, S., Strazielle, C., Lianos, P., *J. Colloid Interface Sci.*, **80**, 208 (1981).
26. Danielsson, I., Lindmann, B., *Colloids Surf.*, **3**, 391, (1981).
27. O'Connor, C. J., Lomax, T. D., Ramage, R. E., *Adv. Colloid Interface Sci.*, **20**, 21 (1984).
28. Albrizzio, J., Archila, J., Rodulfo, T., Cordex, E. H., *J. Org. Chem.*, **37**, 871 (1972).
29. O'Connor, C. J., Lomax, T. D., Ramage, R. E., in *Solution Behaviour of Surfactants* (Ed. by Mittal, K. L., Fendler, E. J.), Plenum Press, New York, **2**, 803 (1982).
30. Kitahara, A., *Adv. Colloid Interface Sci.*, **12**, 109 (1980).
31. El Seoud, O. A., Martins, A., Barbur, L. P., de Silva, M. J., Aldrigue., W., *J. Chem. Soc.*, Perkin Trans., **2**, 1674 (1977).
32. Robinson, B. H., Steytler, D. C., Tack, R. D., *J. Chem. Soc., Faraday Trans. I*, **75**, 481 (1979).
33. Thomas, J. K., *A. C. S. Monograph*, Washington D. C., 184 (1984).
34. Fernandez, M. S., Formherz, P., *J. Phys. Chem.*, **81**, 1755 (1977).
35. Mittal, K. L., Lindman, B., in *Surfactants in Solution*, Plenum Press, New York, **1, 2** (1984).
36. Daiz-Garcia, M. E., Sanz-Model, A., *Atlanta* **33**, 255 (1986).

37. Otsuka, K., Terabe, S., Chromatogr, J. A., **875**, 163 (2000).
38. Pileni, M. P., Nimham, B. W., Gulik-Krzywicki, T., Tanori, J., Lisiecki, I., Filancambo, A., *Adv. Mater.*, **11**, 1358 (1999).
39. Jana, N. R., Gearheart, L., Murphy, C. J., *Chem. Commun.*, 617 (2001).
40. Pal, T., Dey, S., Jana, N. R., Pradhan, N., Mandal, R., Pal, A., Beezer, A., Mitchell, J. C., *Langmuir*, **14**, 4724 (1998).
41. Dey, S., Pal, T., Pal, A., *Langmuir*, **16**, 6855 (2000).
42. Dey, S., Pal, T., Pal, A., Jana, N. R., *J. Photochem. Photobiol. A.* **131**, 111 (2000).
43. Pal, T., Ghosh, T. K., Pal, A., *Ind. J. Chem.*, **40 B**, 850 (2001).
44. Mallick, K., Jewrajka, S., Pradhn, N., Pal, *T., Curr. Sci.*, **80**, 1408 (2001).
45. Pal, T., Jana, N. R., *Langmuir*, **12**, 3114 (1996).
46. Lianos, P., *J. Chem. Phys.*, **89**, 5237 (1988).
47. Evesque, P., *I. Phys.* (Paris), **44**, 1217 (1987).
48. Blumen, A., Klafter, J., Zumofen, G., *Fractals in Physics*, Pietronero, L., Tosatt, E., Eds., North Holland, Amsterdam, 399 (1986).
49. Jana, N. R., Gearheart, L., Murphy, C. J., *J. Phys. Chem.*, **B 105**, 4065 (2001).
50. Heartley, G. S., Roe, J. W., *Trans. Faraday Soc.*, **36**, 101 (1940).
51. Mukherjee, P., Banerjee, K., *J. Phys. Chem.*, **68**, 3567 (1964).
52. Montal, M., Gitler, C., *Bioenergetics,* **4**, 363 (1973).
53. Cassidy, M. A., Warr, G. G., *J. Phys. Chem.*, **100**, 3237 (1996).
54. Saroja, G., Samanta, A., *Chem. Soc. Faraday Trans.*, **92**, 2697 (1996).
55. Laguitton, Pasquier, H., Pansu, R., Chauvet, J. P., Pernot, P., Collet, A., Faure, J., *Langmuir*, **13**, 1907 (1997).
56. Karukstis, K. K., Frazier, A. A., Loftus, C. T., Tuan, A. S., *J. Phys. Chem.*, **B 102**, 8163 (1998).
57. Novaki, L. P., O. A., El Seoud, *Langmuir*, **16**, 35 (2000).
58. Suratkar, V., Mahapatra, S., *J. Colloid Interface Sci.*, **225**, 32 (2000).
59. Pal, S. K., Mandal, D., Bhattacharya, K., *J. Phys. Chem.*, **B 102**, 11017 (1998).

60. Das, P. K., Chaudhury, A., *Langmuir,* **15**, 8771 (1999).
61. Bunton, C. A., Nome, F., Quina, R. H., Romsted, L. S., *Acc. Chem. Res.*, **24**, 357 (1991).
62. Romsted, L. S, Bunton, C. A., Yao, J. H., *Curr. Opin. Colloid Int. Sci.*, **2**, 622 (1997).
63. Romsted, L. S, *J. Phys. Chem.*, **89**, 5107(1985).
64. Romsted, L. S, *J. Phys. Chem.*, **89**, 5113(1985).
65. De Giorgio, V., Corti, M., *Physics of Amphiphiles, Micelles, Vesicles and Microemulsions*, Eds. North-Holland, Amsterdam, (1985).
66. Zana, R., Ed., *Surfactant Solutions: New Methods of Investigation*, Marcel Dekker, New York, (1986).
67. Cardinal, J. R., Mukerjee, P., *J. Phys. Chem.*, **82**, 1614(1978).
68. Mukerjee, P., Ber. Bunsen-Ges., *J. Phys. Chem.*, **82**, 931 (1978).
69. Mukerjee, P., Cardinal, J. R., *J. Phys. Chem.*, **82**, 1620 (1978).
70. Almgren, M., Grieser, F., Thomas, J. K., *J. Am. Chem. Soc.*, **101**, 279 (1979).
71. Lianos, P., Viriot, M. L., Zana, R., *J. Phys. Chem.*, **88**, 1098 (1984).
72. Viaene, K., Verbeek, A., Gelade, E., De Schryver, F. C., *Langmuir*, **2**, 456 (1986).
73. Healy, T. W., White, L. R., *Adv. Colloid Interface Sci.*, **9**, 303 (1978).
74. Formherz, P., Kotulla, R., Ber. Bunsen-Ges., *J. Phys. Chem.*, **88,** 1106 (1984).
75. Drummond, C. J., Grieser, F., Healy, T. W., *J. Phys. Chem.*, **92,** 2604 (1988).
76. Drummond, C. J., Grieser, F., Healy, T. W., *Faraday Discuss. Chem. Soc.*, **81**, 95 (1986).
77. Drummond, C. J., Warr, G. G., Grieser, F., Ninham, B. W., Evans, D. F., *J. Phys. Chem.*, **89,** 2103 (1985).
78. Drummond, C. J., Grieser, F., *Langmuir*, **3**, 855 (1987).
79. Drummond, C. J., Grieser, F., White, L. R., Murray, B. S., *J. Phys. Chem.*, **92,** 5586 (1988).

80. Riddick, J. A., Bunger, W. B., *Techniques of Organic Chemistry, Organic Solvents*, Wiley Interscience, New York, **2**, 592 (1970).

81. Van Uitert, L. G., Haas, C. G., *J. Am. Chem. Soc.*, **75**, 541 (1953).

82. Harned, H. S., Owen, B. B., *The Physical Chemistry of Electrolyte Solutions*, Reinhold, New York, 3rd Edn., (1958).

83. Drummond, C. J., Grieser, F., Healy, T. W., *J. Chem. Soc. Faraday Trans. 1*, **85**, 37 (1989).

84. Sanchez-Ruiz, J. M., Llor, J., Cortijo, M., *J. Chem. Soc. Perkin Trans. 2*, 2047 (1984).

85. Critchfield, F. W., Gibson, J. A., Hall, J. L., *J. Am. Chem. Soc.*, **75**, 1991 (1953).

86. Lamm, G., Pack, G. R., *J. Phys. Chem.*, B, **101,** 9589 (1997).